Fentanyl Detection and Quantification Using Portable Infrared Absorption Spectroscopy

by

Margo Ramsay
B.Sc., University of Victoria, 2018

A Thesis Submitted in Partial Fulfillment of the
Requirements for the Degree of

MASTER OF SCIENCE

in the Department of Chemistry

Fentanyl Detection and Quantification Using Portable Infrared Absorption Spectroscopy

by

Margo Ramsay
B.Sc., University of Victoria, 2018

Supervisory committee

Dr. Dennis K. Hore, Supervisor
(Department of Chemistry)

Dr. Chris Gill, Departmental Member
(Department of Chemistry, Vancouver Island University)

ABSTRACT

Community drug checking is a harm reduction strategy that is currently being employed in response to the ongoing overdose crisis in North America. The Vancouver Island Drug Checking Project uses a variety of methods to analyze drug samples including fentanyl and benzodiazepine immunoassay test strips, attenuated total reflection Fourier transform infrared spectroscopy, Raman spectroscopy and gas chromatography–mass spectrometry. A study was designed to examine the combined ability of infrared spectroscopy and partial least squares regression to quantify the fentanyl content of illicit opioids. Binary and ternary mixtures of powdered fentanyl HCl, anhydrous caffeine and sugar alcohols were prepared as standards representative of the opioids samples presented for drug checking. The infrared spectra of each set of standards was used to train and test individual partial least squares regression models. A grid search was employed to optimize the number of latent variables and data pre-processing strategy for each model. A robust partial least squares regression model, trained on all four sets of standards, was shown to accurately quantify fentanyl content. This model was then used to evaluate the fentanyl concentration of samples brought in for drug checking. In the period October 2018 to December 2020, the detected level of fentanyl in opioid samples had a mean concentration of 10% with a standard deviation of 7%.

Illicit opioids which contained caffeine hydrate were discovered upon examination of the anomalous service samples that were identified by local outlier factor. The infrared spectrum of caffeine shows subtle changes upon its hydration, which are due to differences in the hydrogen bonding pattern of the two forms of caffeine. Standards containing semi-hydrated caffeine and fentanyl HCl were prepared and analyzed to explore the effect of caffeine hydration on fentanyl quantification.

Contents

List of Figures

List of Tables

List of Symbols and Definitions

symbol	definition
HIV	human immunodeficiency virus
PWUD	people who use drugs
TEDI	Trans European Drug Information
NPS	new psychoactive substances
GC–MS	gas chromatography–mass spectrometry
LC–MS	liquid chromatography–mass spectrometry
MS	mass spectrometry
HPLC	high performance liquid chromatography
UV-Vis	ultraviolet-visible
TLC	thin-layer chromatography
ATR	attenuated total reflection
IR	infrared
FTIR	Fourier-transform infrared
SERS	surface-enhanced Raman scattering
SIF	safe injection facility
FTS	fentanyl test strips
BC	British Columbia
USA	United States of America
PWID	people who inject drugs
PCA	principal component analysis
PLSR	partial least squares regression
TIR	total internal reflection
DP	data pre-processing
VIP	variable importance in projection

SNV	standard normal variate
MSC	multiplicative scatter correction
ALS	asymmetric least squares
RMSECV	variable importance in projection
RMSEP	variable importance in projection
r^2_{cv}	correlation coefficient of cross-validation
r^2_{p}	correlation coefficient of prediction
% error	relative error
LARS	least angle regression
LV	latent variables
LoB	limit of blank
LoD	limit of detection
LoQ	limit of quantification
LOF	local outlier factor
μ_G	geometric mean
$\cdots$	hydrogen bond

ACKNOWLEDGEMENTS

I would like to thank my supervisor, Dr. Dennis Hore, for his unwavering support and encouragement throughout this project. Working on this project has been one of the most eye-opening, important and challenging experiences of my life. I am also incredibly grateful to Dr. Bruce Wallace for introducing me to the field of harm reduction and for all the wisdom and guidance he has provided me. I couldn't imagine completing this degree without Lea Gozdzialski, Piotr Burek, Ashley Larnder and Jarred Aasen. Thank you for being the insightful, inspiring and hilarious people you are. A huge thank you to all the team members of the Vancouver Island Drug Checking Project for the joy and support they provided me throughout this process.

This project was funded by a grant from the Health Canada Substance Use and Addictions program, with additional support from the Vancouver Foundation. High performance computing support and server resource allocation was provided by the University of Victoria, WestGrid, and Compute Canada. Abdelhakim Qbaich provided assistance with the implementation of some of the tools. Belaid Moa provided valuable feedback on the optimization of the tools. Rebecca Hof (University of Victoria Centre for Advanced Materials and Related Technologies) provided assistance in the preparation of the binary mixtures. We also thank our community partners Island Health, AVI, and SOLID.

Chapter 1

Introduction

1.1 Drug Checking as a Harm Reduction Service

Although there is no universally accepted definition of harm reduction, it can be described as "a set of practical strategies and ideas aimed at reducing negative consequences associated with drug use. Harm reduction is also a movement for social justice built on a belief in, and respect for, the rights of people who use drugs" [1]. It "focuses on positive change and on working with people without judgement, coercion, discrimination, or requiring that they stop using drugs as a precondition of support" [2]. Needle exchange programs that were introduced as a measure to stop the transmission of blood-borne viruses including hepatitis C and human immunodeficiency virus (HIV) among people who inject drugs are a good example of a harm reduction strategy [1].

1.1.1 Global Drug Checking Projects

Drug checking is a harm reduction service used globally, that allows people who use drugs (PWUD) and others to access chemical analysis for the purpose of identifying components in drug mixtures [3–5]. Europe has a long history of drug checking; the Drug Information and Monitoring System, the first European drug checking service was established in 1992 in the Netherlands [4, 5]. Drug checking services were originally designed for and by recreational drug users in nightlife settings including clubs and festivals [3–5]. The focus of these harm reduction services is to reduce the acute toxicity associated with recreational

drug use since the composition, dose and adulteration of illicit substances can be incredibly variable in unregulated markets [3–5]. A global review reported that there were thirty-one drug checking services operating in twenty countries as of 2017 [3]. The majority of the services were located in Europe, however, drug checking was also on-going in North and South America and Australasia [3].

1.1.2 Options for Service Implementation

The setting, the drug analysis methods, reported wait times for service users and the communication of results differ greatly amongst global drug checking services. With regards to the setting, on-site, fixed-site and postal methods of submission were reported. On-site settings, including festivals and nightclubs, and fixed-site settings, including offices and outreach centres, were both frequently operated whereas only three services offered a postal submission option [3]. The drug analysis methods employed by the services varied drastically; some technologies were integrated into point-of-care services while others required highly skilled technicians and/or a laboratory setting. Mass spectrometry, the current gold standard in forensic drug analysis or liquid chromatography methods were utilized by fifteen of 31 projects surveyed in 2017 [3, 6]. Commonly used technologies, including gas chromatography–mass spectrometry (GC–MS), liquid chromatography–mass spectrometry (LC–MS) and high performance liquid chromatography (HPLC), can very accurately identify and quantify a wide variety of compounds in mixtures [3, 6]. However, these technologies generally require a laboratory setting, have large upfront costs and ongoing operational costs, and require significant expertise to operate [6].

Spectroscopic methods, including infrared (IR) absorption and Raman spectroscopy, are techniques that can accurately and easily perform qualitative analysis for a wide variety of substances [6]. As of 2017, eleven drug checking services around the world were utilizing at least one of these spectroscopic techniques, and or ultraviolet-visible (UV-Vis) spectroscopy [3]. Quantitative analysis using spectroscopy is possible, however,

the feasibility of this should be assessed on a case to case basis. For example, portable infrared (IR) and Raman spectrometers, which can be used in on-site settings, can offer quantitative analysis with high precision comparable with laboratory instruments, but significant expertise is required as the devices do not perform this task automatically [7].

Thirteen global drug checking services reported using thin layer chromatography (TLC) as an analysis technique [3]. TLC can be used to identify a range of illicit substances, however, this technique does not perform well when encountering complex mixtures or novel psychoactive substances [6]. As well, measured retention factors are not unique to a single compound, so TLC is most useful when used in conjunction with another technique [6].

Colorimetric reagent tests were used by sixteen of thirty-one services globally, with four services reportedly using only this drug analysis technique [3]. Colorimetric tests exist for most drugs of abuse, and the reagents are inexpensive, readily available and easy to use [6]. The accuracy of the results can be improved by using a smartphone to identify the resultant colour since each individual perceives colour differently and lighting conditions vary depending on the setting [6]. The utility of this technique is greatly reduced when drugs are present in mixtures, since a single reagent can only test for the presence or absence of a drug or class of drugs. As well, the resultant colours can vary depending on the concentration, the form of the drug (salt vs free base form) and the presence of cutting agents. [6] Overall, reagent tests are simple to use but their accuracy is inconsistent.

Given the diversity of drug analysis methods employed globally it is unsurprising that the reported wait time for service users (the time required to wait for the analysis results) was also quite variable. In general, on-site drug checking services had the shortest turnaround times, followed by fixed-site and postal services, with median wait times of 15–29 minutes, 1–3 days and greater than 7 days respectively [3]. The delivery of the results was also quite varied; both the person(s) to whom the results were reported as well as how the results themselves were communicated. All services reported that

individual service users received their results directly, with the majority of services also communicating results to the public, health/welfare/outreach organizations, researchers and/or promoters/event managers [3]. Certain services also reported their results to the media, politicians and the police. Results were most often communicated in person, however, email, websites, aggregate reports and phone calls were also used by various services [3].

The legal landscape of a particular country and the intended goals of drug checking services, that can range from point-of-care testing to the monitoring of national or global drug trends, will influence the choice of setting, analysis method, reported wait time and communication of results. There are many options to consider with regards to service design and the choices will affect the extent of harm reduction offered by a service.

1.1.3 Support and Criticism of Drug Checking

European drug checking services have been operating for over 25 years and are considered an efficient way of reducing the harm to recreational drug users. The information and advice provided by drug checking services is believed to be more effective at inducing positive and preventive behaviour changes than the promotion of complete abstinence or government-advocated messages [4].

Drug checking can also be used to facilitate public health responses, monitor drug market trends and the emergence of novel psychoactive substances (NPS), compounds designed to mimic existing recreational drugs [4,5]. Trends of interest include the presence of misrepresented compounds, high dose samples and unexpected drug combinations. Market monitoring by the Trans European Drug Information (TEDI) project showed that the adulteration of the European ecstasy market by NPS including mephedrone and methylone increased steadily between 2008–2013 [5]. This finding was significant as there were multiple deaths attributed to mephedrone and methylone during the same time period [8].

Despite the proven benefits and many arguments in their favour, these projects have also received a lot criticism. Opponents of drug checking have claimed that these services could provide people with an unjustified sense of safety regarding their drug use [4]. However, if services commit to providing unbiased scientific information including general risks associated with drug use, this concern is easily addressed. Another common criticism is that drug checking could encourage people to use drugs more frequently or at a higher dosage than originally intended. However, the introduction or presence of a drug checking service in a country does not lead to an increase in drug use [4]. As well, people who accessed these services showed a similar degree of drug use relative to PWUD who did not access drug checking services [4].

1.1.4 Overdose Crisis

Most recently, drug checking has garnered interest as a public health intervention to address the ongoing overdose crisis in North America [9–11]. In Canada, the public health response has been multi-faceted, with strategies such as naloxone distribution, safe injection facilities (SIF) and opioid agonist therapy. Community-based overdose prevention responses including overdose education and naloxone distribution first emerged in the 1990's and remain incredibly vital interventions today [12]. Insite, the first government sanctioned safe injection facility in Canada opened in 2003, however, SIFs have only recently been accepted as crucial harm reduction services [13]. This changing political landscape and the ongoing overdose crisis have led to rapid expansion of SIFs across the country, there were 37 federally sanctioned facilities in 2020 [14].

While many factors contribute to the ongoing crisis, the introduction of synthetic opioids, such as illicitly manufactured fentanyl, to the heroin market plays a significant role [12, 15]. Fentanyl and analogues have been involved in approximately 87% of illicit drug overdose deaths in the Canadian province of British Columbia (BC) which declared overdose to be a public health emergency in 2016. In BC, as in many regions

across North America, the opioid market is saturated with fentanyl. A 2017/2018 drug checking pilot project at two safe consumption sites in Vancouver, BC found that 90.6% of the purported heroin samples tested positive for fentanyl but only 17.6% of these samples actually contained heroin [16]. By contrast, only 5.9%, 2.1%, and 0% of amphetamine/methamphetamine, cocaine and psychedelic samples tested positive for fentanyl respectively [16]. This finding has important public health implications since people who of use stimulants and psychedelics are generally opioid naive, making an overdose scenario much more likely with fentanyl involved. As well, this finding can be used to help dispel the belief that fentanyl is present in all types of illicit substances.

Due to the drug of choice, people who use opioids are at an elevated risk of fentanyl exposure, and this population has distinct differences from the recreational drug users previously targeted by global drug checking services. Recent studies have shown this population (and people who inject drugs) to be diverse in terms of age, race and sex, however, they often lived in precarious housing or experienced homelessness [17–21]. The factors contributing to the overdose crisis and problematic substance use are multifaceted, but should not be considered a specific failing of the individual. However, acknowledging that this population can face much more criminalization and stigma than the general public is important, and past traumatic experiences in a number of settings should be considered [20]. A participant of a pre-implementation survey conducted by the Vancouver Island Drug Checking Project described an upsetting experience within Canada's healthcare system as follows; "Because the moment they find out you're an addict they treat you like shit. So, it's not good. It's like people still need healthcare too. We're not like a diseased rabid animal, you know?" [20]. Therefore, careful consideration should be given to the location and staffing of drug checking services in order for there to be meaningful service uptake. Of primary importance is that staff are skilled technicians who interact with service users in a respectful and judgement free manner [20].

1.1.5 Early Drug Checking Projects Using Fentanyl Test Strips

It is within this context that fentanyl immunoassay strips have increasingly been integrated within overdose responses. The off-label adaptation of fentanyl test strips for drug checking has been adopted as a low-barrier, inexpensive drug checking strategy [17–19, 21, 22]. The intended use of fentanyl test strips (FTS) was for the detection of fentanyl and/or norfentanyl, its major metabolite, in urine [23]. FTS can provide rapid results regarding the presence or absence of fentanyl and several analogues: carfentanil, butyryl fentanyl, p-fluoro fentanyl, acetyl fentanyl, furanyl fentanyl, valeryl fentanyl, ocfentanil, 3-methyl fentanyl, remifentanil, sufentanil and norfentanyl [23]. However, the test strips cannot distinguish between fentanyl and its analogues, nor can they provide information regarding the concentration of fentanyl detected.

In the United States of America (USA), where safe injection facilities and on-site drug checking services are not currently possible due to federal legislation, harm reduction efforts have been significantly limited. However, many organizations have been pursuing the distribution fentanyl test strips for use off-site as a harm reduction intervention [17–19,21,22]. Multiple studies have examined the utility of distributed fentanyl test strips for PWUD or people who inject drugs (PWID) [17–19, 21, 22]. Early studies from Insite in Vancouver and multiple cities across America (data collection: 2016–2017) found that a positive FTS result often led to behaviour changes regarding drug use [17, 19, 22, 24]. It is important to consider whether the use of FTS was carried out prior to drug use or afterwards, as many studies offered both methods [17,19,22,24]. The pre-consumption use of FTS, by dissolving a small portion of the drug in water, was preferred among PWUD [22]. Post-consumption methods, included participants testing their urine or drug residue from bags, spoons or crushed pills [22]. People who received a positive test strip result prior to their drug use were much more likely to report changes in their drug use behaviour compared with post-consumption FTS use [19, 24]. The metrics used to assess drug use behavioural changes differed between studies, including using less than usual, using in

the presence of others, pushing the syringe plunger slower than usual, administering a tester shot, snorting instead of injecting and disposing of the substance [17, 19, 22, 24]. The disposal of drugs was much less frequently reported compared to other behavioural changes [17, 19, 22, 24]. However, in a harm reduction focused service the disposal of drugs may not be a valuable metric since an overarching goal of harm reduction is meeting people where they are at in terms of their substance use and not encouraging or requiring that they stop using drugs [1, 2].

As illicit fentanyl increasingly becomes the ubiquitous opioid, the utility and uptake of test strips is questionable as the presence of fentanyl is assumed and likely unavoidable [24–26]. A more recent study of people who use opioids in Baltimore (data collection: 2018–2019) reported the belief that the opioid market is saturated with fentanyl was widespread [21]. Study participants currently believe that avoiding fentanyl is nearly impossible, however, most participants also described their transition to fentanyl use as unintentional [21]. This example highlights the ever-changing nature of the opioid crisis; it has and will continue to evolve as the availability of and people's preference for certain illicit substances changes.

1.1.6 Instrument-Based Drug Checking

Acknowledging the vital yet limited role of fentanyl test strips, a number of community drug checking projects in Canada and the United States are pursuing the potential role of various instrumental methods of analysis including infrared absorption, Raman scattering, GC–MS, and LC–MS in combination with test strips as a more robust drug checking intervention [10, 11, 16, 27, 28]. In Canada, multi-instrumental drug checking services that offered on-site testing, allowing results to be delivered in a matter of minutes, used a combination of FTS and spectroscopic techniques [29]. Spectroscopic techniques have many advantages; they can identify a wide variety of substances, require minimal sample preparation, are non-destructive, have short run-times and relatively affordable portable

instruments are commercially available [3, 6, 10, 16, 27]. Portable spectrometers based on mid–IR, near–IR and Raman, have been shown to collect spectra of comparable quality to laboratory spectrometers [7]. These spectrometers had good identification and discrimination capabilities when combined with appropriate spectral libraries and principal component analysis (PCA) [7]. Excellent quantitative analysis of solid and liquid samples was achieved with the use of multivariate analysis techniques, namely PLSR [7]. Mass spectrometry (MS) techniques, were employed in two different manners by Canadian drug checking services. MS techniques can be used for secondary validation of the on-site results or as the only technique(s) [29]. However, since the MS techniques often require analysis to be performed off-site in laboratories the results are delayed, usually by a few days [29]. Recent developments in the field of MS show considerable promise with respect to point-of-care drug checking applications, paper spray mass spectrometry is capable of accurately and rapidly quantifying fentanyl analogues and pharmaceuticals in illicit drug samples [30].

Point-of-care drug checking services have been operating in safe consumption sites in Vancouver since 2017, using fentanyl test strips and attenuated total reflection–Fourier-transform infrared (ATR-FTIR) spectroscopy to provide clients with information regarding drug composition [16, 26, 31, 32]. This has enabled the determination of the sensitivity, specificity and limit of detection (LoD) for fentanyl in illicit opioids, in a "real world" setting. Sensitivity describes the ability of a test to correctly identify samples that contain an analyte of interest. It is defined as the number of true positives divided by the total number of true positives and false negatives. Specificity is the ability of a test to correctly identify samples that do not contain the analyte. It is formally defined as the number of true negatives divided by the total number of true negatives and false positives. Ti *et al.* found that FTS had a sensitivity of 87.5% and specificity of 95.2% whereas FTIR spectroscopy had a sensitivity of 72.1% and specificity of 99.0% [32]. The LoD for fentanyl in illicit opioid samples was also assessed for FTS and FTIR spectroscopy, the presence of fentanyl was consistently detected by the fentanyl test strips when the fentanyl concentration was

above 5%, and by FTIR spectroscopy when the fentanyl concentration was above 10% [31]. However, both technologies were capable of detecting fentanyl when its concentration was as low as 1% [31]. The authors proposed that this varying LoD is strongly influenced by the sample composition, for example the presence of caffeine masks fentanyl FTIR signals [31].

A multi-city study from the USA assessed the LoD of fentanyl for three drug checking techniques: FTS, ATR–FTIR and Raman spectrometers. The Raman spectrometer was used in two modes: point and shoot & surface-enhanced Raman scattering (SERS) [27]. The FTS LoD reported by this study was 0.100–0.150 μg/mL, much lower than that reported by drug checking services in Vancouver, however, this was assessed on solutions of fentanyl standards not illicit opioid samples [27]. The reported LoD for the FTIR spectrometer and SERS was 3–4% by weight and 25 μg/mL respectively [27]. The assessment of the devices sensitivity and specificity for fentanyl was performed on seized drug samples which were intended for end-user consumption. Multiple types of drugs were analyzed including opioids containing fentanyl and analogues, heroin, cocaine, methamphetamine and various pharmaceutical substances. Green *et al.* found that FTS had the highest sensitivity and specificity, $\geq$ 96.3% and $\geq$ 90.4% for both laboratories [27]. Overall, the Raman spectrometer had high specificity but inadequate sensitivity, the use of SERS improved the sensitivity significantly for one study location [27]. Infrared spectroscopy was only used in Rhode Island, where they found the sensitivity and specificity to be 83.3% and 90.2% respectively [27]. The authors also suggested sample composition and its variability to be a contributing factor for the inconsistency in stats reported by the two locations included in the study [27]. Table 1.1 summarizes the LoD, sensitivity and specificity for fentanyl detection as reported by several studies.

Overwhelmingly, the early findings from community drug checking pilot projects point to the need to pursue drug checking technologies and techniques that can exceed test strips confirmation of fentanyl to provide PWUD with estimates of concentration and potency to

Instrument	Location	LoD	Sensitivity	Specificity
Fentanyl Test Strips	Vancouver	1-5% w/w	87.5%	95.2%
Fentanyl Test Strips	Baltimore	0.150 µg/mL	100%	98.1%
Fentanyl Test Strips	Rhode Island	0.100 µg/mL	96.3%	90.4%
FTIR	Vancouver	1-10% w/w	72.1%	99.0%
FTIR	Rhode Island	3-4% w/w	83.3%	90.2%
Raman – point & shoot	Baltimore	--	3.8%	98.1%
Raman – point & shoot	Rhode Island	--	3.7%	100%
Raman - SERS	Baltimore	--	38.5%	92.3%
Raman - SERS	Rhode Island	25 µg/mL	61.1%	91.5%

Table 1.1: Statistical comparison of fentanyl detection by current drug checking techniques

advise safer use [31–33]. North American drug checking services have been pursuing this goal by using FTS in combination with a portable spectrometer or by accessing laboratory analysis using MS techniques. The accurate quantitative information that MS can provide that is very desirable but the longer wait time could seriously negate the harm reduction benefits for the individual service user. As European drug checking projects have shown MS can still be incredibly informative with respect to drug market monitoring and public health responses.

1.1.7 Vancouver Island Drug Checking Project

The Vancouver Island Drug Checking Project in collaboration with the local health authority, has been operating a free, confidential drug checking service in Victoria, BC since 2018. The selected locations for drug checking included safe injection/consumption sites and community outreach centers in downtown Victoria. Drug samples are analyzed using a variety of methods including fentanyl and benzodiazepine immunoassay test strips

(BTNX), ATR–FTIR spectroscopy, Raman spectroscopy of powders and SERS using colloidal gold nanoparticle solutions, and GC–MS. Since the service was designed to offer point-of-care drug checking at multiple locations, the selected technologies were all portable.

1.2 ATR–IR Spectroscopy

Spectroscopy is the study of the interaction between electromagnetic radiation and matter. Modern spectroscopic techniques can make use of many types of electromagnetic radiation for this purpose, including X-rays, visible light, infrared light, and radio waves. In an absorption experiment the quantities that can be obtained are typically the transmittance or reflectance, depending on the sample and beam geometry. Both quantities are defined with respect to the intensity $I_0(\nu)$ measured with a reference sample or black in order to eliminate the frequency (ν)-dependent contributions from the electromagnetic source and the detector to the spectral response [34]. $I_{\mathrm{T}}(\nu)$ and $I_{\mathrm{R}}(\nu)$ are the intensity of light that has transmitted through or has reflected from the sample respectively.

$$T(\nu) = \frac{I_{\mathrm{T}}(\nu)}{I_0(\nu)} \tag{1.1}$$

$$R(\nu) = \frac{I_R(\nu)}{I_0(\nu)} \tag{1.2}$$

When light encounters an interface between two non-absorbing media (the refractive indices are real), it can be reflected or transmitted. How the incident light interacts with the interface depends on physical parameters such as the angle of incidence and material properties including the refractive indices of the two media. The real part of the refractive index, n, describes how fast light travels through of a material with respect to the speed of light in a vacuum, c. If medium 1 has a lower refractive index than medium 2, $n_1 < n_2$, then medium 1 and medium 2 are called the optically rarer and optically denser medium respectively. With regards to reflection there are two general cases to be considered: external and internal reflection. Fig. 1.1a shows the case of external reflection, which occurs

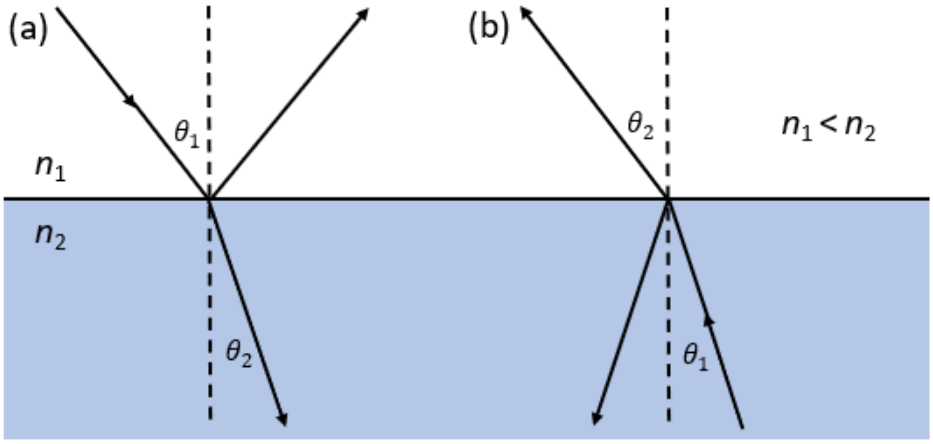

Figure 1.1: Light interacting with an interface between two non-absorbing media, θ_1 and θ_2 are the incident and refracted angles respectively. (a) External reflection occurs when light is incident from the rarer medium and (b) internal reflection occurs when light is incident from the denser medium.

when the light is incident from the optically rarer medium to the interface with a material having a larger refractive index, such as when sunlight propagating through air encounters the ocean's surface. Internal reflection, Fig. 1.1b, occurs when the light is incident from the optically denser medium to the interface with a material with a smaller refractive index, such as when light travelling through glass encounters the glass-air boundary.

$$n_1 \sin\theta_1 = n_2 \sin\theta_2 \tag{1.3}$$

In the case of internal reflection, if medium 2 is transparent there exists a critical angle for which there is no transmission and the entire power of the incident beam is reflected. The phenomenon that occurs when the incident angle is equal to or greater than the critical angle, θ_c, and the incident beam is entirely reflected is known as total internal reflection (TIR).

$$\sin\theta_c = \frac{n_1}{n_2} \tag{1.4}$$

For TIR there is no transmitted beam, instead in the rarer medium there is an evanescent wave that penetrates into the rarer medium and decays exponentially with distance from the interface [34, 35]. The penetration depth of the evanescent wave is dependant on the

wavelength of light as shown by Eq. 1.5 [34, 35]. The penetration depth is also dependant on the angle of incidence and the refractive indices of the two media.

$$d_p = \frac{\lambda}{2\pi\sqrt{n_1^2 \sin^2\theta - n_2^2}} \tag{1.5}$$

For absorbing media, the refractive index is complex with real and imaginary parts, $N = n + i\kappa$, where κ is the extinction coefficient for the electric field amplitude, representing the attenuation of the electromagnetic wave as it propagates through the material. Put simply, the imaginary part of the refractive index is related to absorption. When there is an absorbing material the interface becomes slightly "leaky" to electromagnetic energy, and some energy crosses the interfaces and is absorbed by the rarer medium [34]. Therefore, the reflected beam no longer carries all the incident electromagnetic energy, the reflection has been attenuated. This phenomenon is known as attenuated total reflection (ATR), the reflected beam contains the IR absorption information of the substance of interest and can be analyzed similarly to transmission IR spectra. ATR spectroscopy measure the absorption of the first few microns of the substance at the interface since the intensity of the evanescent wave decays exponentially with distance from the reflection surface.

Compared to transmission infrared spectroscopy, ATR has some distinct advantages. Traditionally, to collect transmission infrared spectra solid samples are crushed and mixed with a non-absorbing material such as KBr, the mixture is then pressed into a clear disk [36]. However, this sample prep is laborious and challenging and sample recovery is not practical. A simpler alternative to KBr pellet making is diffuse reflection spectroscopy, where samples are ground and mixed with KBr but analyzed using reflection spectroscopy [36]. The reflected spectrum has dips at wavelengths where the sample absorbs light, similar to transmission spectroscopy [36]. ATR by contrast can be used for the sampling of solids and liquids and the substance of interest is placed directly on the ATR accessory which makes sampling much more convenient and sample recovery is easy. Since the penetration depth of the evanescent wave is dependant on the wavelength of light, Eq. 1.5,

ATR spectra should be transformed by at least the simple ATR correction of $1/\lambda$ in order to be comparable with transmission spectra.

1.3 Aims and Objectives

The objective of this work is to demonstrate the use of data from a portable ATR–FTIR spectrometer in combination with PLSR to build a chemometric model capable of predicting fentanyl content in relevant drug mixtures. A framework will be presented for the quantification of fentanyl in samples analyzed by our drug checking service. The limitations of such a model will be considered both analytically and with respect to a harm reduction service.

Chapter 2

Methods

2.1 Preparation of Standards

Powder fentanyl HCl, heroin (Toronto Research Chemicals), anhydrous caffeine, mannitol, erythritol, inositol and dextrose (Sigma-Aldrich) were used to prepare standards that were representative of illicit opioids. Binary mixtures of fentanyl HCl and caffeine ranging from 1–40% fentanyl were prepared by combining stock solutions of fentanyl HCl and caffeine in chloroform. All reported percentages will be with respect to the total weight of the mixture. The solutions were evaporated using a benchtop concentrator (Labconco CentriVap), and then plasma cleaned steel balls (Bearings Canada) were added to the binary mixtures and the dry solid was vortexed until a powder mixture was achieved. Ternary mixtures of fentanyl HCl, caffeine and heroin, ranged from 1–20% fentanyl and 5–20% heroin. Ternary mixtures of fentanyl HCl, caffeine and mannitol, ranged from 1–20% fentanyl and 10–40% mannitol. Ternary mixtures of fentanyl HCl, caffeine and erythritol, ranged from 1–20% fentanyl and 10–40% erythritol. Stock solutions of fentanyl HCl, caffeine and heroin were prepared in chloroform; mannitol and erythritol solutions were made in deionized water. The solutions were dried by the concentrator, the powders were re-suspended in pentane in an effort to increase sample homogeneity, and then dried by concentrating once again.

Hydrated caffeine was prepared by combining the anhydrous caffeine with an equal amount of sterilized water, and then the slurry was mixed in a mortar and pestle for 5

minutes and left out to dry overnight. This hydrated caffeine was then combined with powdered fentanyl HCl and mixed in a mortar and pestle to create the hydrated binary standards.

2.2 Spectral data acquisition and analysis.

The infrared spectra were obtained with a portable FTIR spectrometer (Agilent Agilent 4500a, Agilent Technologies, Santa Clara, California, USA) equipped with a dTGS (deuterated triglycine sulphate) detector and a diamond ATR accessory. ATR–FTIR data were collected by co-adding 32 scans over the 650–4000 cm^{-1} range at a spectral resolution of 4 cm^{-1} and zero fill factor of 4. Custom scripts, including those that make use of Scikit-learn [37] Python packages, were used to perform the following statistical analyses: partial least square regression, least angle regression, variable importance in projection, and local outlier factor analysis.

2.3 Partial Least Squares Regression

ATR–FTIR spectroscopy has been used in combination with chemometrics, a group of techniques and operations associated with the mathematical manipulation and interpretation of chemical data across many disciplines. When the analysis goal is the quantification of a compound of interest, partial least squares regression (PLSR) is a commonly used multivariate statistical analysis method [38]. PLSR is a factor-based regression method that projects the predictor (typically referred to as the X matrix) and response (the Y matrix) variables to a latent variable space, while maximizing the covariance between the two variables [38]. The PLSR algorithm calculates X-scores, which are estimates of the latent variables and loadings, the weights that transform the original X variables to the X-scores and builds a predictive calibration model using these X-scores and loadings [38, 39]. ATR–FTIR spectroscopy and PLSR have been successfully used in food sciences for quality control and to monitor for product adulteration for a variety of compounds: phenolic

compounds in olive oils, various sugars in honey, and the fatty acid content in Omega-3 supplements [39–41]. Within the field of drug analysis this combination, ATR–FTIR and PLSR, has been implemented for many purposes including the quantification of Penicillin V during fermentation, doping drugs bambuterol and terbutaline in urine, and of cocaine and adulterants in seized cocaine samples [42–44]. However, in these cases the samples were analyzed as liquids [39, 40, 42, 43] or when the samples were in solid phase the analytes of interest were present in significant quantities [41, 44]. When active ingredients and cutting agents are both powders, it is challenging to account for the heterogeneity that results from incomplete mixing. Furthermore, when the actives are present at quantities below approximately 10% w/w, additional challenges arise due to the small contribution to the total absorbance, ultimately impacting the limit of detection.

2.4 Optimization of PLSR models

A typical chemometric analysis involves 5 steps: data acquisition, data pre-processing, variable reduction, modeling and model evaluation [45]. Despite the widespread application of chemometrics to spectroscopic data, and the knowledge that data pre-processing is a crucial step in the analysis there remains no set of guidelines for optimizing the choice of pre-processing [45–50]. Pre-processing methods transform raw data to "clean" data by removing unwanted variation, however, if the incorrect methods are selected variation can be added and the resultant model worsened [45, 47, 48, 50]. A 2017 review of data pre-processing for ATR–FTIR spectroscopy found that pre-processing was not consistently used and when it was the authors rarely explained their choice of methods [45]. One reason for this gap of knowledge is that the optimal pre-processing is dependant both on the data and the goal of the data analysis [48, 49]. Additionally, a wide variety of pre-processing techniques are available, and multiple techniques can be applied successively [45–50]. Therefore, for simplicity we will refer to the application of a single pre-processing technique or a combinations of techniques as the data pre-processing (DP) strategy [45].

Engel et al. examined three common methods for choosing a DP strategy (trial and error, visual inspection and quality parameters) and found "they may be time-consuming beyond practicability or may provide misleading results" [48]. Recent works have tried to improve and simplify the selection of a DP strategy by using design of experiments or "super" parameters, by combining multiple quality parameters together [46, 47, 50]. In this work a hybrid approach will be used to optimize the PLSR model, by combining the trial and error approach and the use of a "super" parameter.

Regarding a PLSR model there are three aspects that should be considered during model optimization: the DP strategy, the number of latent variables and the spectral range to be used. Of these, the latter is the least critical since the PLSR model will weight to the original spectrum so that frequencies that co-vary with the response variable are enhanced. However, the variable importance in projection (VIP) of a PLSR model built from the raw data was used reduce the spectral range to relevant frequencies, which slightly improved the overall model performance.

The spectral range was set to 650–3250 cm^{-1} while optimizing the remaining two aspects at once. It is widely accepted that cross validation should be used to determine the optimal number of latent variables to be used [38]. After consulting literature nine pre-processing techniques appropriate for ATR–FTIR spectroscopy were shortlisted, and similar techniques were grouped. The scatter corrections and normalization techniques considered were area normalization, vector normalization, min/max normalization, standard normal variate (SNV) and multiplicative scatter correction (MSC). The baseline corrections and derivative techniques considered were asymmetric least squares (ALS) baseline correction, rubberband baseline correction, first derivative (Savitzky-Golay smoothing, window size 5, polynomial order = 2) and second derivative (same smoothing parameters).

One pre-processing technique from each of the two groups of techniques, scatter corrections & normalization and baseline corrections & derivatives, were combined

Scatter / Normalization	Baseline / Derivative
A – Area normalization	F – Asymmetric least squares baseline
B – Vector normalization	G – Rubberband baseline
C – Min/max normalization	H – 1st derivative (S-G smoothing, window = 5, polynomial order = 2)
D – Standard normal variate	I – 2nd derivative (S-G smoothing, window = 5, polynomial order = 2)
E – Multiplicative scatter correction	Z – No pre-processing
Z – No pre-processing	

Table 2.1: Data preprocessing techniques and their short codes.

exhaustively for a total of fifty different DP strategies, their short codes are shown in Table 2.1. To assess the effect of DP strategies on the PLSR model performance, parameters such as the root mean square error of cross validation (RMSECV) and/or root mean square error of prediction (RMSEP) are generally used [40, 42, 46, 51]. However, using only RMSECV and RMSEP may not lead to the best model. Therefore, we will also be considering the correlation coefficient of cross-validation (r^2_{cv}) and prediction (r^2_p), as well as the relative error (% error) when assessing the model performance. We propose that calculating the geometric mean

$$\mu_G = \sqrt[5]{\text{RMSECV} \cdot (1 - r^2_{cv}) \cdot \text{RMSEP} \cdot (1 - r^2_p) \cdot \frac{\%\text{error}}{100}} \tag{2.1}$$

of the normalized values of the five parameters can help to shortlist appropriate DP strategies.

2.5 Compound identification.

Least angle regression (LARS) algorithm was used to identify what substances have been used as cutting agents. A custom IR library was created by collecting the ATR-IR spectra of standards of suspected opioid drug sample components: fentanyl HCl, heroin, anhydrous caffeine, mannitol, erythritol, sorbitol, inositol, xylitol, lactose and dextrose. This custom IR library was compared to the IR spectra of 741 service samples that were known to

contain fentanyl and/or an analogue. Known fentanyl content was ascertained by a positive fentanyl test strip result. The LARS algorithm fit linear regression models to the spectra of opioid samples, and returned an estimate of the components in the samples.

The cut-off values for acceptable matches were decided upon by analyzing standards of known composition using LARS. When the binary standards were analyzed by LARS caffeine was always identified as the first component. Fentanyl was consistently identified as the secondary component for standards with concentrations $\geq 3\%$, the LARS coefficient values for these matches were 0.02. From this analysis the decision was made to set the cut-off value for acceptable residual matches at 0.03.

Chapter 3

Fentanyl Quantification

3.1 Introduction

Our project operates within a context in which 95% of opioids are confirmed to be fentanyl and caffeine is the most common (96%) substance combined with these fentanyl samples [52]. A 2020 study of harm reduction sites in BC showed that fentanyl exposure was recognized among PWUD, and a significant number of people were knowingly using fentanyl [26]. Individuals bringing illicit opioid samples for drug checking therefore expect the presence of fentanyl in their supply, and are seeking information regarding the potency of their drugs.

Fig. 3.1 shows the ATR–IR spectra of anhydrous caffeine and 15% fentanyl in caffeine standards. Even when a significant proportion of fentanyl is present the infrared spectrum on illicit samples is dominated by caffeine features. The most distinctive absorption bands for fentanyl occur around 710 cm^{-1}, which are C–H wagging modes of the two mono-substituted aromatic rings in the structure of fentanyl [53,54]. The similarity of the caffeine and fentanyl IR spectra hinders the identification of fentanyl in illicit samples, likely a contributing factor to the high LoD for fentanyl reported by drug checking projects in Vancouver.

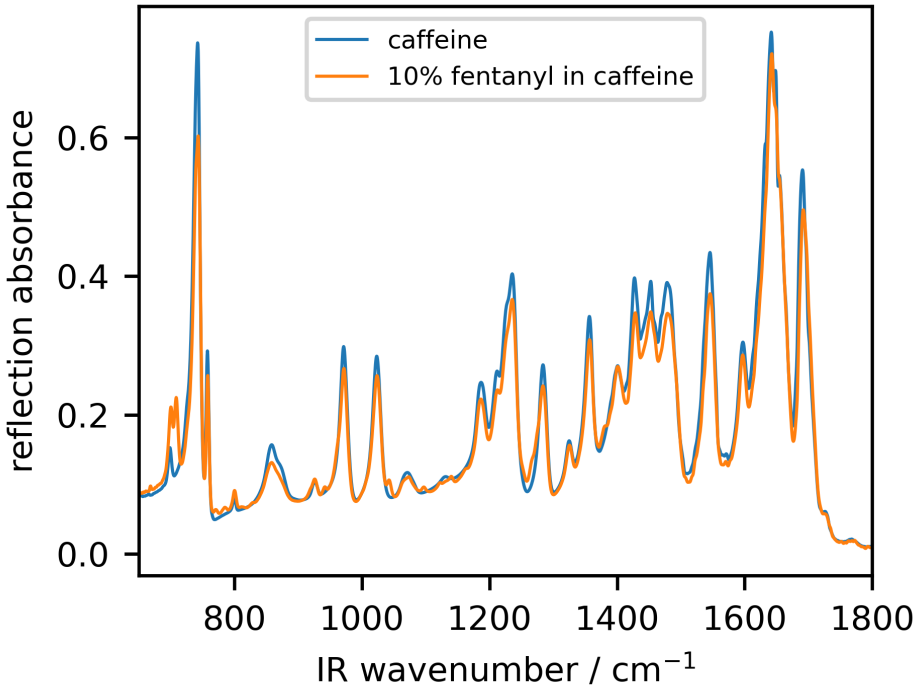

Figure 3.1: Overlay of the ATR–FTIR spectra of a caffeine standard and a 15% fentanyl in caffeine standard.

3.2 Tailored PLSR Models

The frequency of eight opioid components identified by the LARS algorithm are summarized in Fig. 3.2. The 741 opioid spectra analyzed by the LARS algorithm were collected between October 2018 and December 2020 by the Vancouver Island Drug Checking Project. Caffeine was the most common cutting agent, it co-occurred in 95.3% of fentanyl positive opioid samples. Mannitol, erythritol and xylitol were also commonly used as cutting agents, occurring in 15.0%, 8.8% and 7.7% of fentanyl positive samples. Heroin was only identified in 12.1% of fentanyl positive samples and was rarely identified in the absence of fentanyl. The remaining cutting agents were seen in less than 5% of fentanyl positive samples.

With regards to optimizing the PLSR models a grid search was employed to find the number of latent variables (in the range 1–15) that minimized the RMSECV value, using

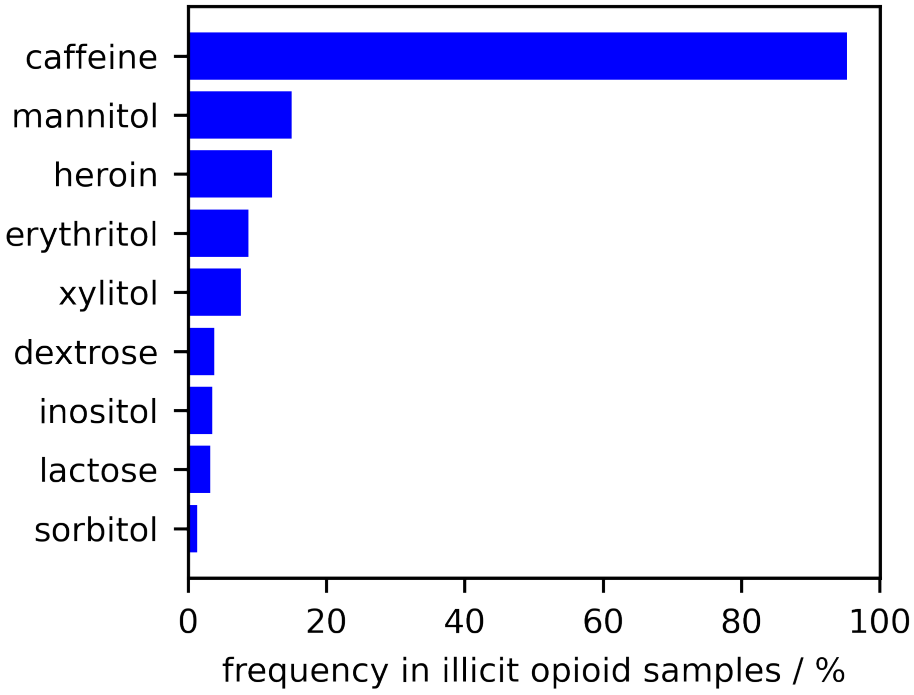

Figure 3.2: Opioid drug sample components, identified by the LARS algorithm, in 741 service samples that contained fentanyl or an analogue.

a 10-fold cross validation, for each of the fifty DP strategies. Then for each DP strategy the corresponding RMSEP, r^2_{cv}, r^2_p, % error and μ_G values were calculated. The results were sorted according to their μ_G value, acceptable models were those with less latent variables (LV) and lower μ_G values than a model (Z, Z) trained on the raw data. The grid search results for the top 10 models and the model built on the raw data for the binary standards are shown in Table 3.1. The first row in Table 3.1 summarizes the parameters of the optimized binary model: DP strategy, number of LV, RMSECV, RMSEP, r^2_{cv}, r^2_p, percent error and μ_G.

Fig. 3.3 shows the accuracy line of the optimized binary caffeine/fentanyl PLSR model with 4 latent variables, area normalization and first derivative (Sav-Gol smoothing, window = 5, order = 2) as the DP strategy. The accuracy line compares the predicted fentanyl concentration with the known fentanyl concentration for binary standards in the test set. The optimized model (A, H) showed significantly decreased predictive error compared to

PLSR Calibration & Test Sets	DP strategy	LVs	r^2_{cv}	RMSECV	r^2_p	RMSEP	% Error	μ_G
Binary	C, F	6	0.977	0.924	0.997	0.557	7.58	0.076
Binary	F, C	6	0.963	0.873	0.997	0.540	7.18	0.080
Binary	F, D	6	0.976	0.897	0.996	0.650	7.09	0.082
Binary	I, A	5	0.924	0.916	0.997	0.543	5.80	0.089
Binary	A, H	4	0.972	0.830	0.996	0.670	10.3	0.092
Binary	A, F	3	0.982	0.826	0.995	0.745	11.9	0.092
Binary	B, F	3	0.955	0.879	0.996	0.644	7.80	0.094
Binary	G, C	6	0.981	0.757	0.993	0.871	8.98	0.095
Binary	C, G	6	0.981	0.758	0.993	0.871	9.01	0.095
Binary	H, C	10	0.972	0.906	0.995	0.771	8.54	0.097
Binary	Z, Z	6	0.965	1.07	0.980	1.50	11.6	0.167

Table 3.1: Results from the grid search for the optimization of the latent variables, and data pre-processing strategy for the binary standards.

the unprocessed model, with RMSEP values of 0.670 and 1.50 respectively, and μ_G values 0.092 and 0.167 respectively. While DP strategies (C, F), (F, C) and (F, D) had comparable μ_G values, these models had the same complexity (6 LV) as the unprocessed model so weren't considered further. One DP strategy (I, A) had decreased model complexity and predictive error with respect to the unprocessed model, but was not selected due to its low r^2_{cv} value of 0.924.

In addition to the caffeine/fentanyl PLSR model, tailored PLSR models were made for each set of standards individually. For example, in the tailored mannitol model only the ternary mannitol/caffeine/fentanyl standards were used for calibration and testing. The number of LV and DP strategy for these models were also optimized using the grid search, the results of which are shown in Table 3.2. The tailored accuracy lines for the heroin, erythritol and mannitol standards are shown in Fig. 3.4, 3.5 and 3.6 respectively. As shown in Table 3.2 the RMSEP was $\leq 1.00\%$ for all of the tailored models, showing that PLSR models can be used to accurately quantify fentanyl in diverse opioid mixtures. For each

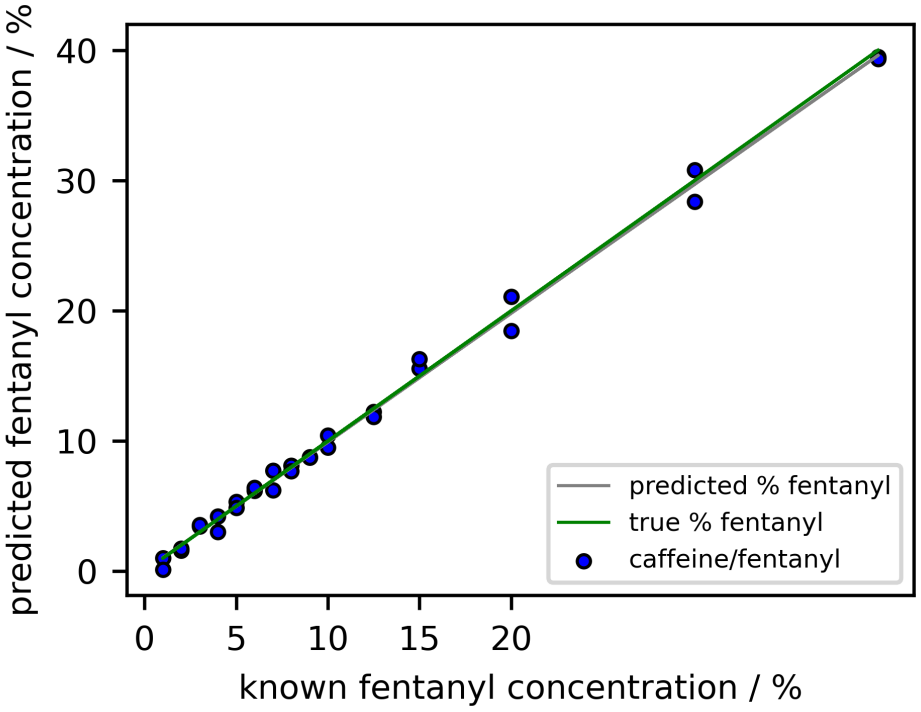

Figure 3.3: Tailored accuracy line for the binary standards. The spectral range of 650–3250 cm^{-1} was selected, 3 and 2 replicates were in the calibration and test sets respectively, and 10 fold cross validation was used.

PLSR Test Set	PLSR Calibration Set	DP strategy	LVs	r^2_{cv}	RMSECV	r^2_p	RMSEP	% Error	μ_G
Binary	Binary	A, H	4	0.972	0.830	0.996	0.670	10.3	0.0920
Heroin	Binary	A, H	4	0.972	0.830	0.944	1.60	30.7	0.230
Erythritol	Binary	A, H	4	0.972	0.830	-0.767	9.03	237	0.974
Mannitol	Binary	A, H	4	0.972	0.830	0.715	3.63	73.8	0.447
Heroin	Heroin	D, H	4	0.934	1.27	0.982	0.922	6.88	0.158
Erythritol	Erythritol	A, F	6	0.977	0.808	0.986	0.806	18.1	0.130
Mannitol	Mannitol	D, F	9	0.980	0.798	0.994	0.537	8.88	0.086
Binary	Robust	F, A	10	0.975	1.10	0.993	0.857	14.9	0.121
Heroin	Robust	F, A	10	0.975	1.10	0.975	1.08	23.4	0.176
Erythritol	Robust	F, A	10	0.975	1.10	0.988	0.760	16.8	0.134
Mannitol	Robust	F, A	10	0.975	1.10	0.970	1.18	15.5	0.171
Binary, Mannitol, Erythritol, Heroin	Robust	F, A	10	0.975	1.10	0.985	0.976	17.0	0.147

Table 3.2: Optimized model parameters for tailored and robust PLSR models.

set of standards a different DP strategies was chosen, interestingly, overall only four pre-processing techniques were selected: area normalization, SNV, ALS baseline correction and 1^{st} derivative (short codes: A, D, F and H respectively). The number of latent variables suggested by cross validation was also inconsistent, ranging from 4, for the binary and heroin standards, up to 9, for the mannitol standards.

There are many sources of uninformative variation and/or spectral artifacts associated with ATR–FTIR spectroscopy that contribute to the prediction error of our regression models. Sources of spectral variability include baseline offsets and slopes, overlapped peaks, light scattering, inconsistent sample sizes, varying particle sizes and particle size distribution and moisture content [45, 48, 49, 55–57]. The optimization of the DP strategy used in the PLSR models can help to remove some variation due to baselines offsets and slopes, overlapped peaks, inconsistent sample sizes and light scattering. However, other types of variation such as mixture heterogeneity are inherent in multi-component powder mixtures, as it is challenging to achieve a perfect mixture of powders.

A 2016 paper showed that the intensity, width and area of bands in the ATR–FTIR

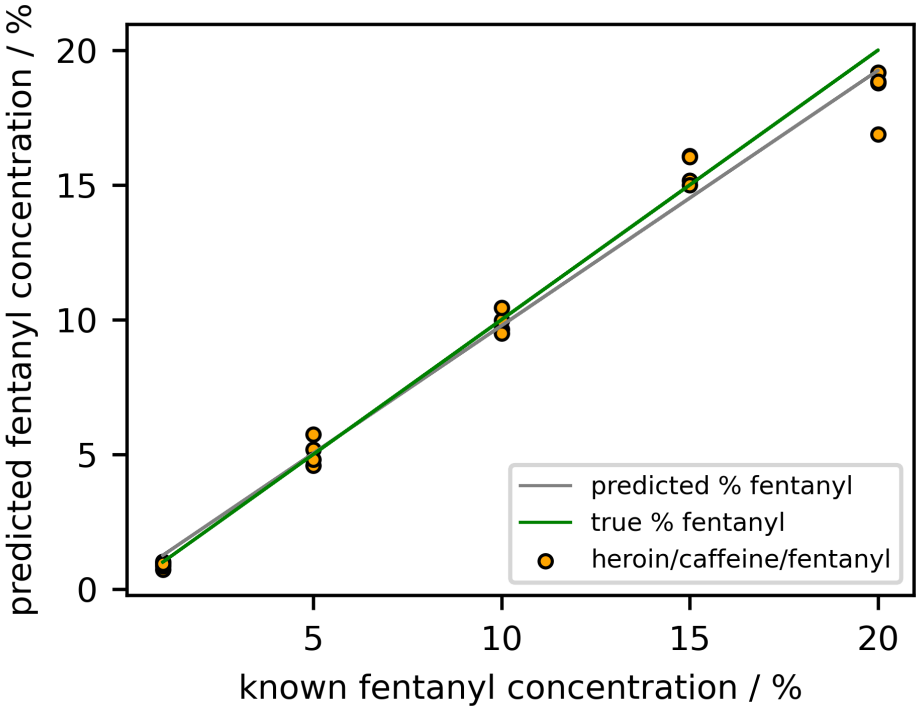

Figure 3.4: Tailored accuracy lines for the heroin standards. The spectral range of 650–3250 cm^{-1} was selected, 3 and 2 replicates were in the calibration and test sets respectively, and 10 fold cross validation was used.

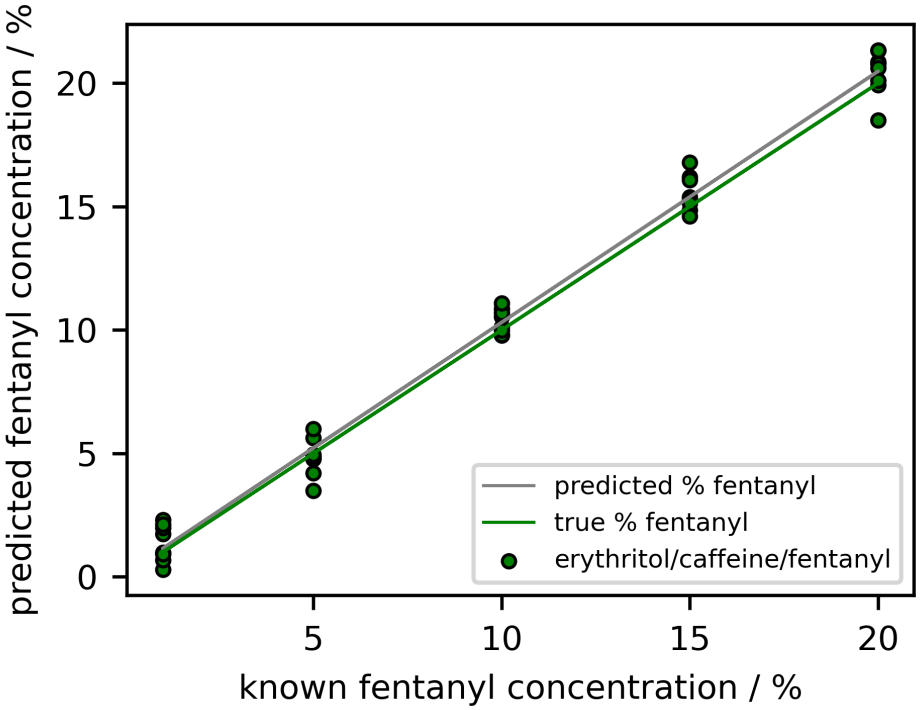

Figure 3.5: Tailored accuracy lines for the erythritol standards. The spectral range of 650–3250 cm^{-1} was selected, 3 and 2 replicates were in the calibration and test sets respectively, and 10 fold cross validation was used.

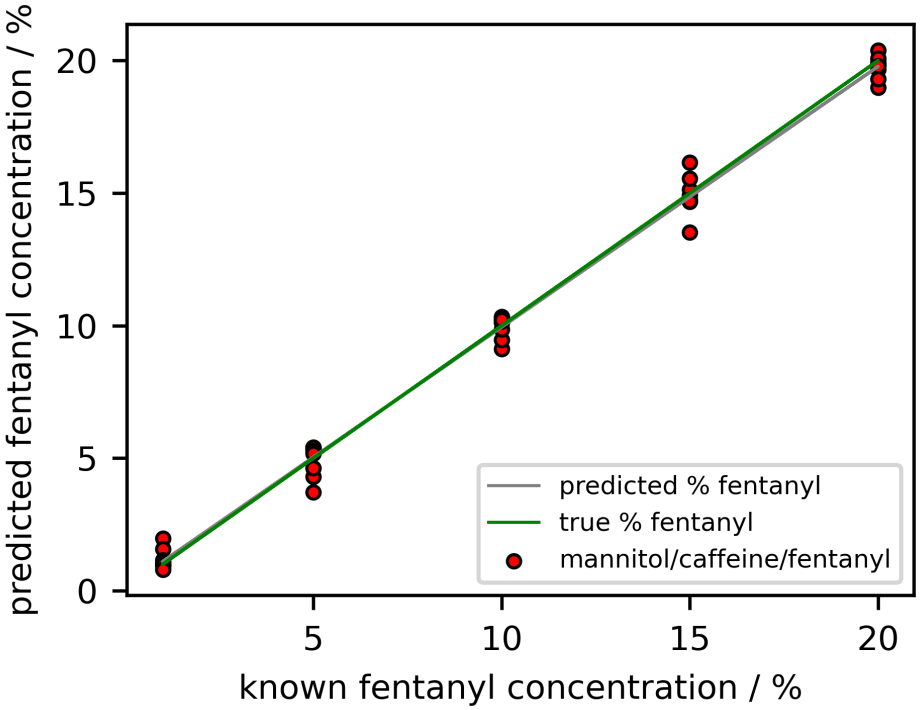

Figure 3.6: Tailored accuracy lines for the mannitol standards. The spectral range of 650–3250 cm^{-1} was selected, 3 and 2 replicates were in the calibration and test sets respectively, and 10 fold cross validation was used.

spectra of mineral powders have explicit dependence on the particle size [57]. The mineral powders were separated into particle size fractions and the ATR–FTIR spectra of each fraction was collected, decreasing the particle size (down to 2–4 μm) resulted in increased intensities and peak areas [57]. Below 2 μm the IR intensity decreased due to the wavelength and penetration depth of the IR light [57]. However, since it is neither practical nor helpful to sieve our standards or illicit opioid samples into distinct particle size fractions the most practical approach is to crush all standards and samples to a consistent and small particle size.

A 2006 paper studying binary mixtures of powders with ATR–FTIR found that it is crucial to consider both the average particle size and the distribution of particle sizes for each of the components in the mixture [56]. If the particle size of one component is significantly smaller than the others this component will be over-represented at the ATR–FTIR interface since the smaller particles can be packed more tightly and will fill the gaps in between the larger particles [56]. However, a component in a powder mixture may also be over-represented if that component has a larger proportion of small particle sizes relative to the other component [56]. This suggests that the accuracy of regression models for powder mixtures is somewhat dependant on the particle sizes and size distributions of all components in the mixture. As well, an accurate regression model would require the samples to be homogeneous mixtures which is challenging to obtain in practice [56]. Therefore, we expect some prediction error despite efforts to optimize the DP strategy.

Fig. 3.7, 3.8 and 3.9 show the accuracy lines of the optimized binary PLSR model when the test set contains only the heroin, erythritol and mannitol ternary standards respectively. The fentanyl predictions for all ternary standards show increased error relative to the binary standards in Fig. 3.3, this is undoubtedly due to the additional component in the sample mixture on which the PLSR model has not been trained. In Fig. 3.8 it can be seen that the fentanyl concentration in the erythritol standards was consistently under predicted, the RMSEP was 9.03% fentanyl. Again in Fig. 3.9 it can be seen that the fentanyl

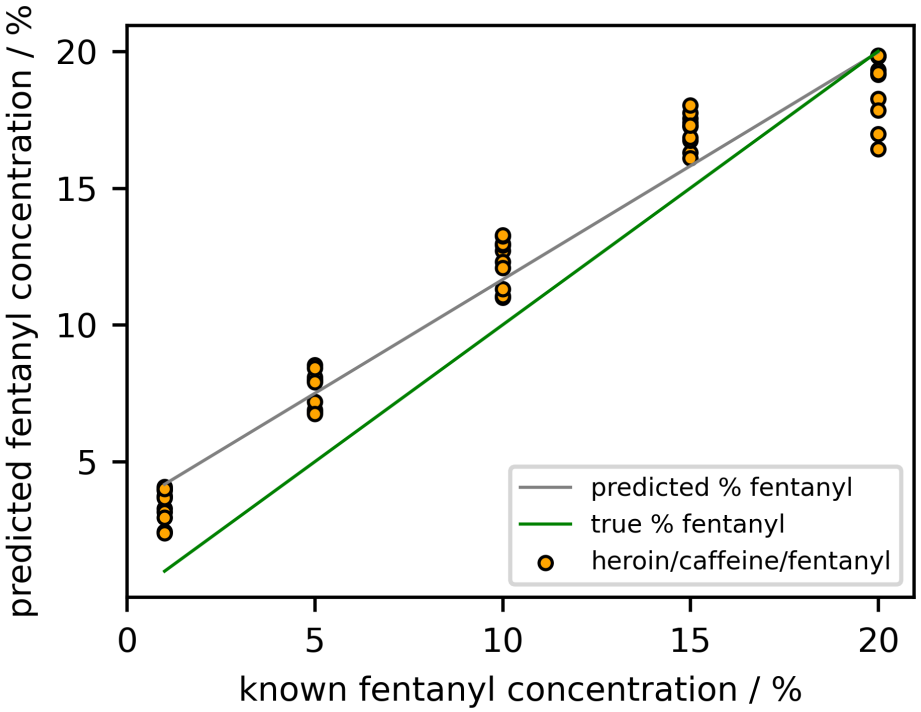

Figure 3.7: Accuracy line for a PLSR model (DP strategy was area normalization + 1st derivative and 4 latent variables) trained on the caffeine/fentanyl calibration set, and tested using the caffeine/fentanyl/heroin standards as the test set. The spectral range of 650–3250 cm^{-1} was selected, 3 and 2 replicates were in the calibration and test sets respectively, and 10 fold cross validation was used.

concentration in the mannitol standards was consistently under predicted, the RMSEP was 3.63% fentanyl. The prediction error for the heroin standards does not show such an obvious trend, Fig. 3.7, in some the predicted fentanyl concentrations are close to accurate while in other the fentanyl concentrations are being over or under predicted, the overall RMSEP was 1.60% fentanyl. The extent of this prediction error depends on the additional component itself, the mannitol standards have a RMSEP of 3.63% fentanyl whereas the erythritol standards have a much larger RMSEP of 9.03% fentanyl. The relative amount of this additional component also has an effect on the models predictions. This can be seen by the vertical spread in the predictions at each known fentanyl concentration in Fig. 3.7, 3.8 and 3.9, since the mannitol and erythritol content was varied (10, 20, 30 & 40%) and the heroin content was varied (5 & 20%) at each known fentanyl concentration.

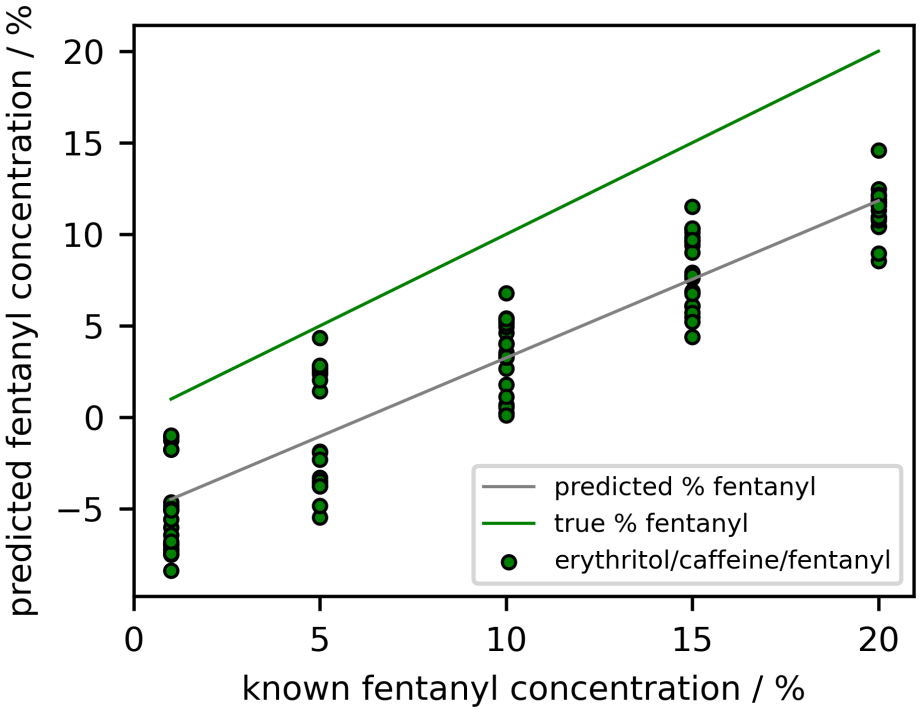

Figure 3.8: Accuracy line for a PLSR model (DP strategy was area normalization + 1st derivative and 4 latent variables) trained on the caffeine/fentanyl calibration set, and tested using the caffeine/fentanyl/erythritol standards as the test set. The spectral range of 650–3250 cm^{-1} was selected, 3 and 2 replicates were in the calibration and test sets respectively, and 10 fold cross validation was used.

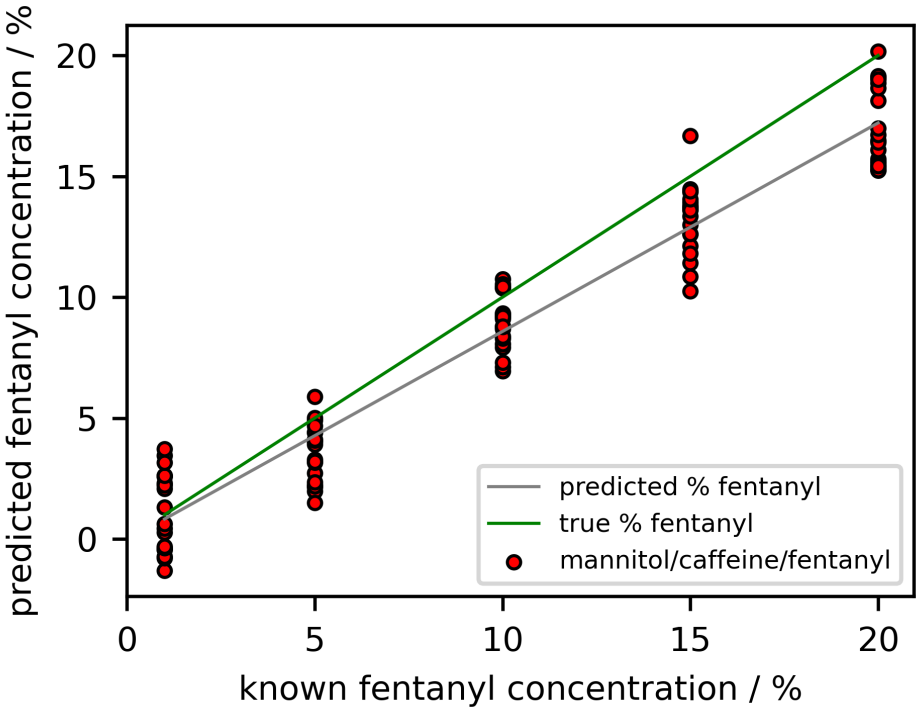

Figure 3.9: Accuracy line for a PLSR model (DP strategy was area normalization + 1st derivative and 4 latent variables) trained on the caffeine/fentanyl calibration set, and tested using the caffeine/fentanyl/mannitol standards as the test set. The spectral range of 650–3250 cm^{-1} was selected, 3 and 2 replicates were in the calibration and test sets respectively, and 10 fold cross validation was used.

The decision to use the fully optimized binary PLSR model to prediction the fentanyl concentration in ternary standards was done to assess the utility of this binary model from a service perspective. A wide variety of components are seen in the illicit opioids in Victoria, however, caffeine is usually the major component. Therefore, we wished to assess if a PLSR model trained only on caffeine/fentanyl binary mixtures would be capable of accurately predicting the fentanyl concentration in more complicated mixtures. As described above, the predictions varied drastically, but overall showed significant inaccuracy. This is especially true when we compare the results to the RMSEP for optimized individual models, as shown in Table 3.2. For example, the optimized erythritol PLSR model has a RMSEP of 0.806% but when the binary model is used to predict the fentanyl concentration in these same samples the RMSEP value is 9.03%. This demonstrates the importance of having a relevant calibration set for our PLSR models, even optimized PLSR models will breakdown, give erroneous predictions, when encountering unfamiliar data.

3.3 Robust PLSR Models.

It is not always possible to reliably identify all the components in an illicit opioid sample, which would be necessary if we were wanting to use tailored PLSR models that match the components seen in a specific sample. For example, if someone were to bring in an illicit opioid sample that contains caffeine, mannitol and fentanyl and these compounds were successfully identified in the ATR–IR spectrum then one would choose to use the mannitol ternary PLSR model to predict the fentanyl concentration, but if the presence of mannitol was missed or it was misidentified as a different carbohydrate then an inappropriate model would be chosen. There are many reasons this could occur, such as if mannitol was the minor component in the mixture or the technician examining the spectrum was inexperienced. From a service perspective it is desirable to have one robust model capable of accurately predicting the fentanyl concentration in a wide variety of opioid samples.

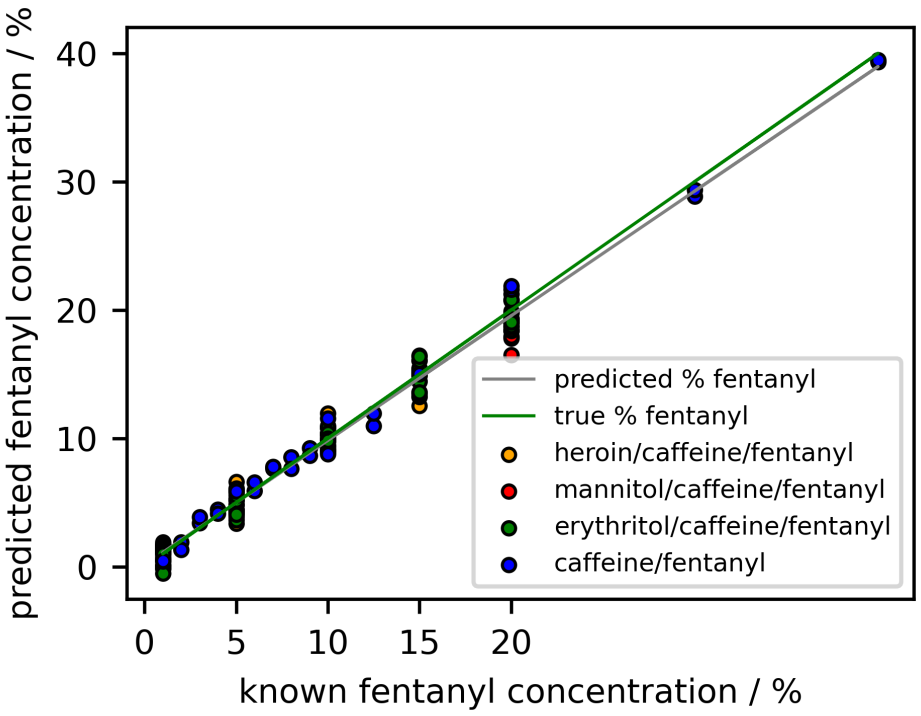

Figure 3.10: Accuracy line for the robust PLSR model (DP strategy was ALS baseline + area normalization and 10 latent variables) trained and tested on all standard sets. The spectral range of 650–3250 cm^{-1} was selected, 3 and 2 replicates were in the calibration and test sets respectively, and 10 fold cross validation was used.

Therefore, we decided to combine all the sets of standards in one PLSR model, known as the robust model, the accuracy line of this model is shown in Fig. 3.10. The optimized model had 10 LVs, used ALS baseline correction and area normalization as the DP strategy and had RMSEP and μ_G values of 0.976, and 0.147 respectively. However, before deciding to use this robust model in service we wanted to compare the accuracy of the predictions when the tailored PLSR model was used vs. when the robust PLSR model was used. The results of this comparison, using the RMSEP since it is the average difference between the known and prediction fentanyl concentrations, are shown in Fig. 3.11. The binary caffeine standards had a RMSEP of 0.670 and 0.857% fentanyl for the binary tailored and robust model respectively. The ternary heroin standards had a RMSEP of 0.922 and 1.08% fentanyl for the ternary heroin tailored and robust model respectively. The ternary erythritol standards had a RMSEP of 0.806 and 0.760% fentanyl for the ternary erythritol

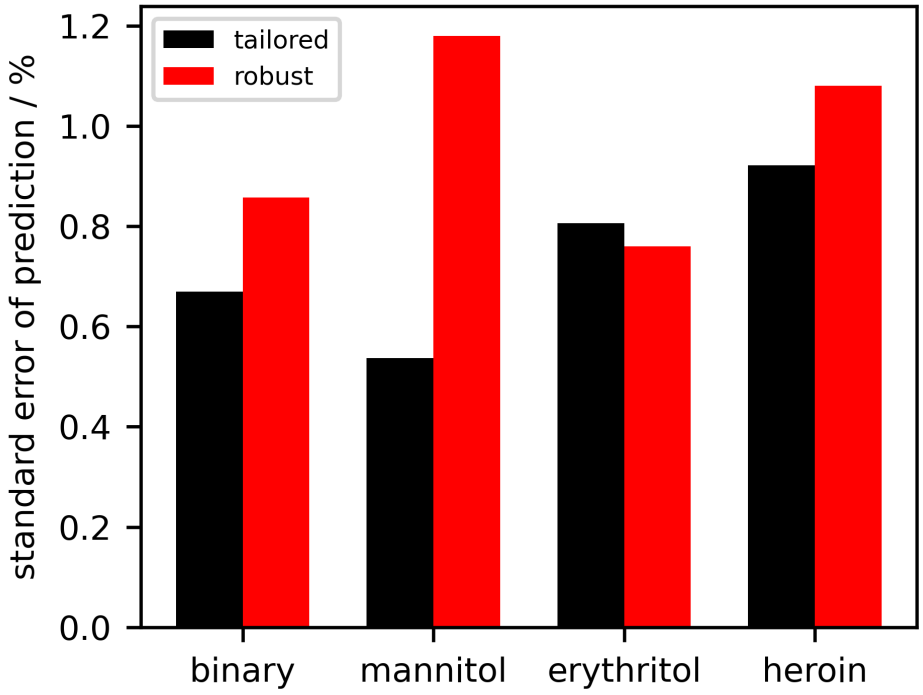

Figure 3.11: Comparison of the root mean standard error in prediction (RMSEP) of fentanyl for the tailored and robust PLSR models for the binary caffeine, ternary mannitol, ternary erythritol and ternary heroin standards.

tailored and robust model respectively. The ternary mannitol standards had a RMSEP of 0.537 and 1.18% fentanyl for the ternary mannitol tailored and robust model respectively. There is an increase in the RMSEP value for three out of four of the sets of standards, we believe that this increase is acceptable from a service perspective. The accuracy of the fentanyl predictions improved slightly for the ternary erythritol standards when the robust model was used. The accuracy of the fentanyl predictions for the ternary mannitol standards showed the largest RMSEP increase when the robust model was used. However, the tailored mannitol model also boasted the smallest RMSECV and RMSEP values of any optimized model and a high degree of model complexity, 9 LVs, which could suggest this model was over-fit.

Table 3.3 shows the limit of the blank (LoB), limit of detection and the limit of quantification (LoQ) for fentanyl for the binary and robust PLSR models respectively.

PLSR Model	Blank	LOB	LOD	LOQ
Binary	Caffeine	-0.53	0.11	3.00
Robust	Caffeine	0.12	0.35	3.00

Table 3.3: Limit of the blank, limit of detection and limit of quantification for the binary and robust models.

Caffeine was used as the blank for both models. The following criteria was used for calculating the limit of quantification: LoQ $\geq$ LoD & % error $\leq$ 10%. When PLSR was used in addition to ATR–IR analysis the limit of detection for fentanyl in illicit opioids was found to be 0.11 and 0.35% for the binary and robust models respectively. The limit of quantification for both models was 3.00% fentanyl.

3.4 Analysis of Opioid Samples Presented for Drug Checking

There are some adulterants, currently circulating within the illicit opioid market, that have psychotropic effects at extremely low concentrations. Xylazine, benzodiazepines, and etizolam have been seen in opioids samples in BC, these depressants compound the respiratory depressant effects of opioids, increasing the risk of overdose and their effects are not reversed by the use of naloxone [58–62]. Reports from Health Canada's Drug Analysis Service show that multiple fentanyl analogues, such as carfentanil, acetyl fentanyl, and furanyl fentanyl, were circulating in 2020 [59–61]. Given the market variability, and the possible presence of low-dose actives, we acknowledge that fentanyl quantification in illicit opioids does not mitigate all risks associated with opioid use.

Fig. 3.12a shows a 2D projection of the X-scores for the second and third latent variables. In Fig. 3.12b, the 741 opioid samples from service (plotted in purple) are included with the standards (same colours as in Fig. 3.12a). Some potentially anomalous samples can seen, such as those with X-score 2 values less than -100 or X-score 3 values greater than 100. Since the service samples represent an independent test set we chose a

novelty detection algorithm known as local outlier factor (LOF). LOF is an unsupervised algorithm that takes into consideration the local deviation of density of a sample with respect to its k-nearest neighbours in the latent variable space. Each sample is given a negative outlier score that represents its degree of abnormality, allowing the exclusion of anomalous samples from further analysis. Based on the LOF analysis of the standards, the decision was made to extend the negative outlier score cut-off value to -2.0, instead of -1.5. The black circles in Fig. 3.12 have radii corresponding to negative outlier scores for the standards and service samples. The X-scores of all 10 latent variables in the robust model are given as input to the LOF algorithm, however, the projection was limited to a two dimensional X-score plot for simplicity.

After excluding the anomalous samples identified by LOF and samples with negative predictions, 425 service samples from October 2018 to December 2020 remained; a plot of the predicted fentanyl concentrations is displayed in Fig. 3.13. Our data show that there was considerable variability in the fentanyl content of illicit samples, fentanyl concentrations up to 34% were predicted. The mean and median fentanyl concentration were found to be 10% and 8% respectively with a standard deviation of 7%.

While the combination of ATR–FTIR spectroscopy and PLSR shows promise in the quantification of fentanyl in binary and ternary mixtures for point-of-care services, the availability of confirmatory testing to validate the fentanyl concentrations would make these findings more robust. Furthermore, we note that only 425 out of 741 service samples (57%) were considered in the quantitative analysis. We have reason to suspect that the large number of outliers may be due, in part, to a lack of standardization of measurement protocols and instrument parameters in our early data when the drug checking service was first established.

Since the onset of the COVID-19 pandemic (estimated as March 2020) there has been an increase of the number of fatal overdoses in BC [63]. Many factors outside of the drug market itself likely have contributed to this spike in fatalities such as the closure and

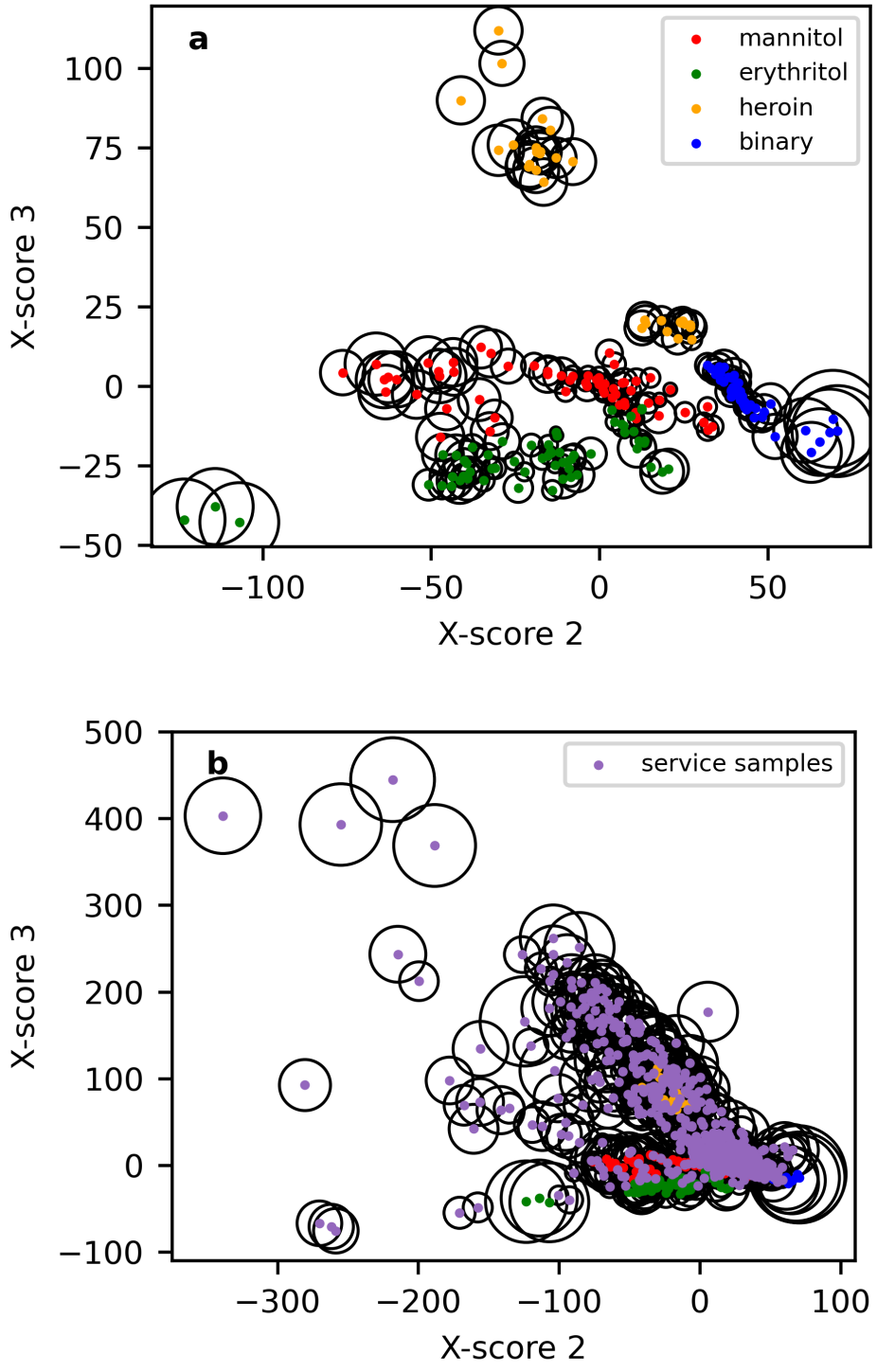

Figure 3.12: 2D projection of the robust X-scores for the second and third latent variables for (a) the binary caffeine, ternary heroin, ternary erythritol, ternary mannitol standards (b) and service samples known to contained fentanyl and/or an analogue. The negative outlier scores, which represents the degree of abnormality of a sample, are shown in black.

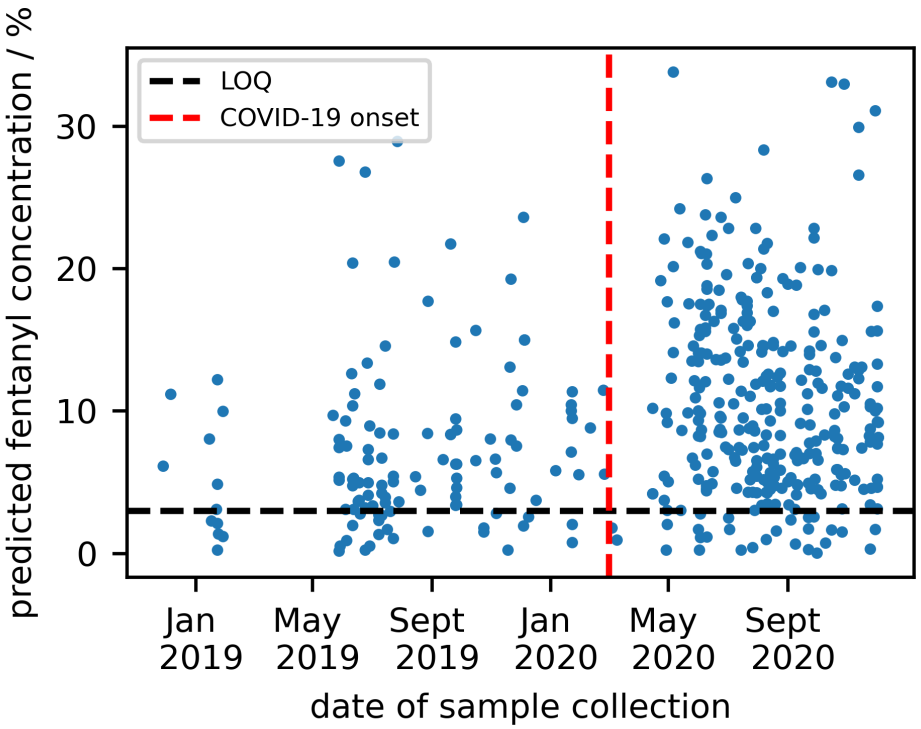

Figure 3.13: Time series of the positive fentanyl concentrations predicted by the robust PLSR model for 425 service samples, after removing the 282 novelties suggested by LOF. The limit of quantification and the onset of the COVID-19 pandemic are shown by the black and red dashed lines respectively.

displacement of safe injection sites, health regulations encouraging social distancing and limiting social gathering—all of which limit important harm reduction measures previously practiced by PWUD. Another potential factor is an increase in the potency of illicit opioids. The mean fentanyl concentration prior to the COVID-19 pandemic was 7% with a standard deviation of 6%, but after the onset the mean increased to 11% with standard deviation of 7%. A similar trend was reported for street samples that were measured by Health Canada's Drug Analysis Service laboratory. In 2019 the mean fentanyl concentration was 9.4% with a standard deviation of 13.7%, whereas in 2020 the mean fentanyl concentration was 16.3% with a standard deviation of 23.0% [64]. Co-occurring with the increase in fentanyl potency was an increase in the adulteration of illicit opioids in BC by depressants including xylazine, etizolam and benzodiazepines. All these factors compound to exasperate and complicate the overdose epidemic, resulting in more preventable deaths.

3.5 Conclusions

Within the context of an unregulated drug market quality control efforts, including PLSR models applied to ATR–IR data for the quantification of fentanyl, can help mitigate some of the risks faced by people who use drugs. A grid search was employed to optimize the number of latent variables and data pre-processing strategy for each model. A robust PLSR model, trained on four sets of standards representative of illicit opioids, was shown to accurately quantify fentanyl content. This model was then used to evaluate the fentanyl concentration of samples brought in for drug checking. In the period October 2018 – December 2020, opioid samples had a mean fentanyl concentration of 10% with a standard deviation of 7%. This demonstrates that portable ATR–IR spectroscopy is suitable for the rapid identification of components in a drug mixture, and can be used to quantify fentanyl in opioid samples, even in challenging cases where a variety of substances are used as cuts.

Chapter 4

Caffeine Hydration and Its Affect on Fentanyl Quantification

4.1 Introduction

Familiarity with the IR spectra of caffeine, fentanyl and sugar alcohols seen in illicit opioids is a great asset when performing point of care drug checking. Visual inspection of a sample's spectrum can allow the technician to 'double check' the fentanyl content suggested by PLSR. As well, this familiarity can help in noticing unique samples at the time they are presented for drug checking. Fig. 4.1 shows the IR spectra of the four types of standards on which the robust PLSR model and LOF were trained. All standards have 15% fentanyl and Fig. 4.1b, c and d are three component mixtures with 20% of heroin, mannitol and erythritol respectively. When heroin is the third component, Fig. 4.1b, many small peaks can be seen throughout the 800–1250 cm^{-1} and 2750–3250 cm^{-1} spectral regions. The presence of mannitol, Fig. 4.1c, or erythritol, Fig. 4.1d, is marked by the appearance of new absorption bands in the 800–1100 cm^{-1} and 2750–3500 cm^{-1} regions. Compared to the spectrum of the binary standard shown in Fig. 4.1a all ternary standards have increased absorption below 750 cm^{-1}. As previously discussed, when fentanyl is mixed with caffeine the most distinctive absorption bands for fentanyl occur around 710 cm^{-1} so an elevated baseline or additional absorption modes in this region can interfere with its identification.

Since we wanted to be cautious to not include inappropriate samples (those different

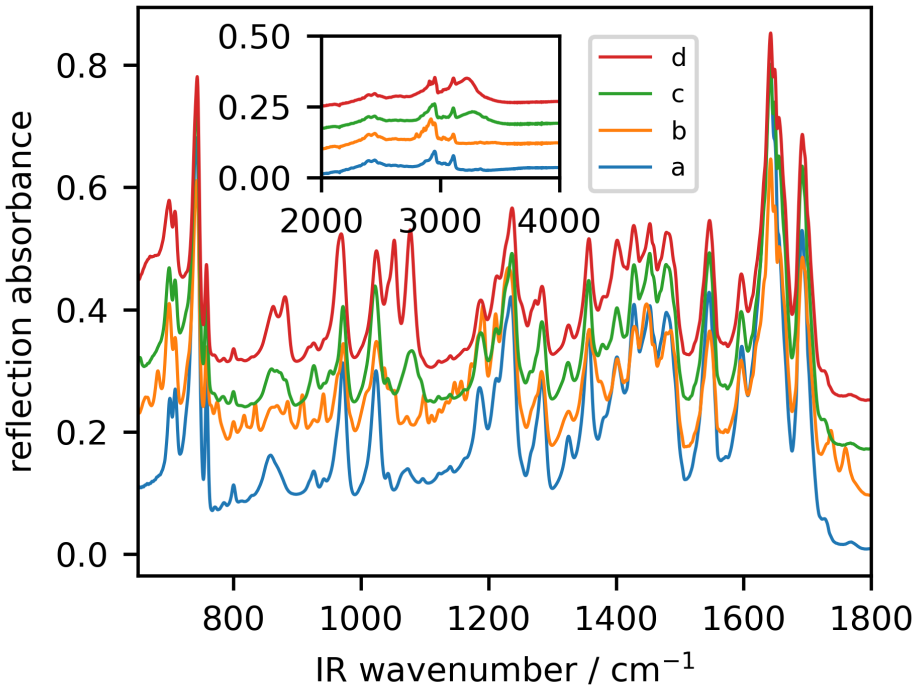

Figure 4.1: Infrared spectra of standards included in the robust PLSR model from 650–1800 cm^{-1}, the spectral region 2000–4000 cm^{-1} is shown in the inset. Shown are (a) a binary standard with 15% fentanyl, (b) a ternary heroin standard with 15% fentanyl and 20% heroin, (c) a ternary mannitol standard with 15% fentanyl and 20% mannitol (d) and a ternary erythritol standard with 15% fentanyl and 20% erythritol.

from the standards on which the PLSR model was trained) in the large scale quantitative analysis of illicit opioid samples in Victoria, local outlier factor was used to determine which samples were appropriate. However, we also did not want to exclude samples unnecessarily so the IR spectra of the 282 samples which were classified as novelties by the LOF algorithm were examined, four of which are shown in Fig. 4.2. Visual inspection confirmed that some of these samples were truly anomalous, such as opioid samples where fentanyl was the major or only component, Fig. 4.2a, and mixtures of sugar alcohols and fentanyl only, Fig. 4.2b. Others had noticeable heroin content, Fig. 4.2c. These types of samples have noticeably different IR spectra from the standards on which the robust PLSR model was trained, and would have likely given erroneous fentanyl predictions. Unlike the previous panels, Fig. 4.2d appears to be a typical illicit opioid except for noticeable water content evidenced by the broad O–H absorption band centered around 3300 cm^{-1}. This 'hydrated' opioid sample appears quite similar to the binary standard shown in Fig. 4.1a, except for the broad O–H stretch and elevated baseline below 750 cm^{-1}.

Water seemed to be quite prevalent in opioid samples presented to the service. Updated results from the LARS analysis are shown in Table 4.3. Water was identified as a component in 17.3% of samples analyzed by LARS, making it the second most common 'cutting agent' in Victoria. It was noticed that these 'hydrated' services samples did not appear to dry even after being crushed and exposed to room temperature air for extended periods of time. This suggested that the water was present as a water of crystallization as opposed to as a component in a slurry.

4.2 Hydration States of Caffeine

Caffeine is a solvate, a material that can incorporate a solvent molecule into its crystal lattice. Recrystallizing anhydrous caffeine in water or mechanochemistry, the use of mechanical forces to induce chemical transformations, can produce the hydrated form of methylxanthines [65]. Grinding caffeine and water in a mortar and pestle for 5 min is

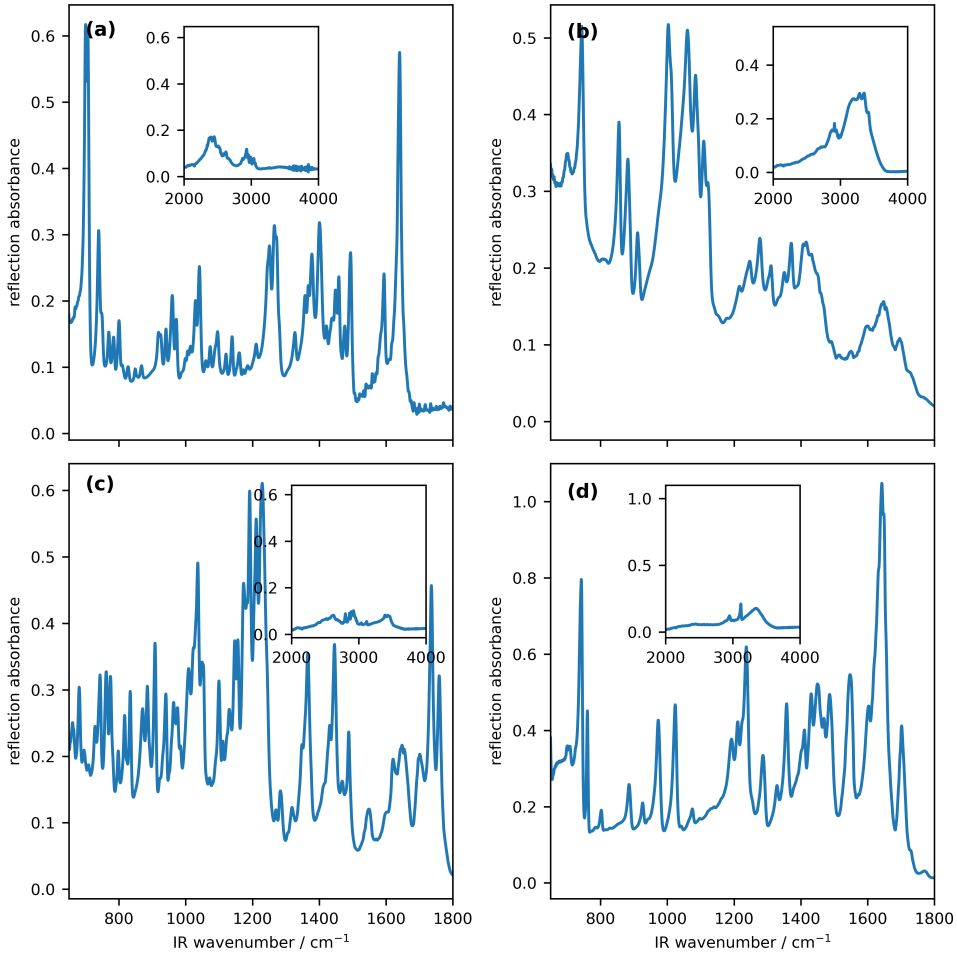

Figure 4.2: Infrared spectra of anomalous samples identified by LOF from 650–1800 cm^{-1}, the spectral region 2000–4000 cm^{-1} is shown in the inset. Shown are (a) a high concentration fentanyl sample, (b) a sample containing xylitol as the only cutting agent (c) a sample with a high concentration of heroin, and (d) a sample with noticeable water content.

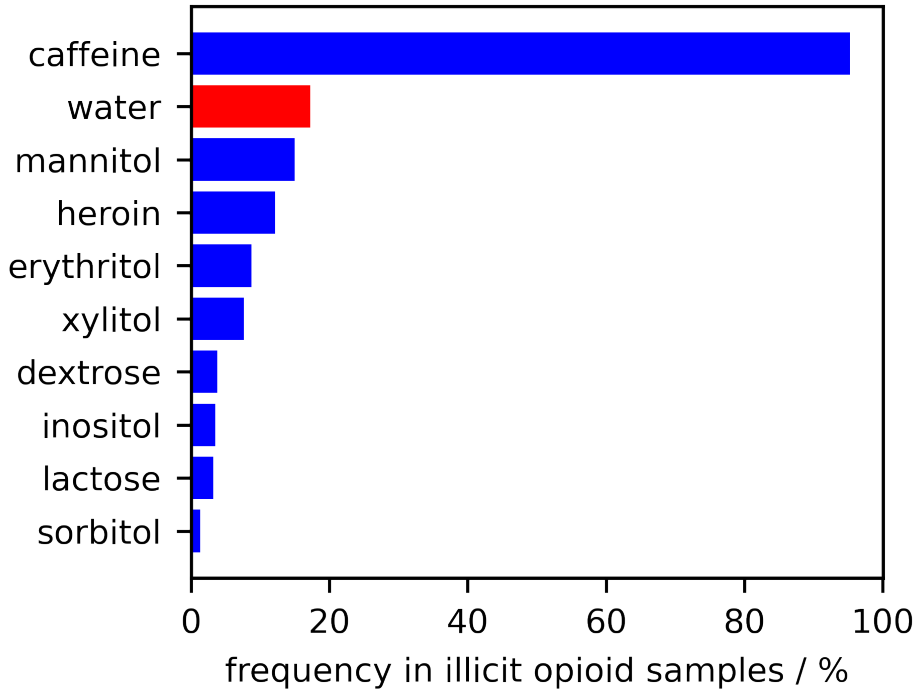

Figure 4.3: Water and opioid drug sample components, identified by the LARS algorithm, in 741 service samples that contained fentanyl or an analogue.

reportedly enough to induce the hydration [65]. Fig. 4.4 shows the chemical structure of caffeine, including the atom numbering of xanthine derivatives. In its anhydrous form caffeine molecules form pairs through the following hydrogen bond, $C_{(8)}$–H$\cdots$$N_{(9)}$ [66]. In its hydrated form the imidazole nitrogen, $N_{(9)}$, forms a strong hydrogen bond with the water of crystallization, $N_{(9)}\cdots$H–O_w [66]. This bond activates the adjacent carbon as a hydrogen bond donor and a hydrogen bond is established with a carbonyl oxygen, $C_{(8)}$–H$\cdots$$O_{(2)}$ [66]. An additional hydrogen bond forms between the other carbonyl oxygen and the imidazole methyl group, $C_{(7)}$–H$\cdots$$O_{(6)}$ [66]. The IR spectra of the anhydrous and hydrated forms of caffeine are quite similar as can seen in Fig. 4.5. The most obvious change is the appearance of the signature broad O–H stretch centered around 3357 cm^{-1} in the spectrum of caffeine hydrate. In the anhydrous form there is a small peak, $\sim$3112 cm^{-1}, assigned to the imidazole $C_{(8)}$–H stretching absorption that is shifted to $\sim$3121 cm^{-1} and shows significantly increased intensity upon hydration [65, 66]. Other spectral changes

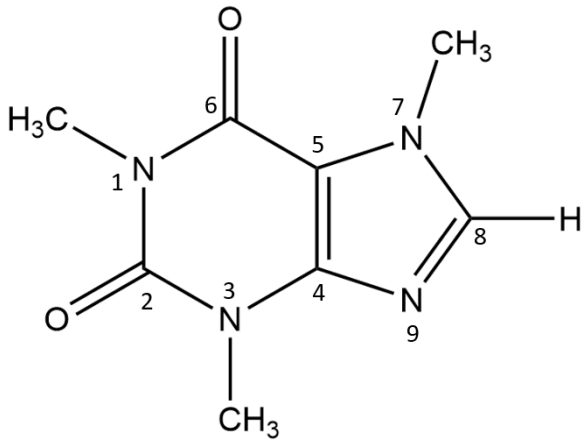

Figure 4.4: Chemical structure of caffeine, including the atom numbering of xanthine derivatives

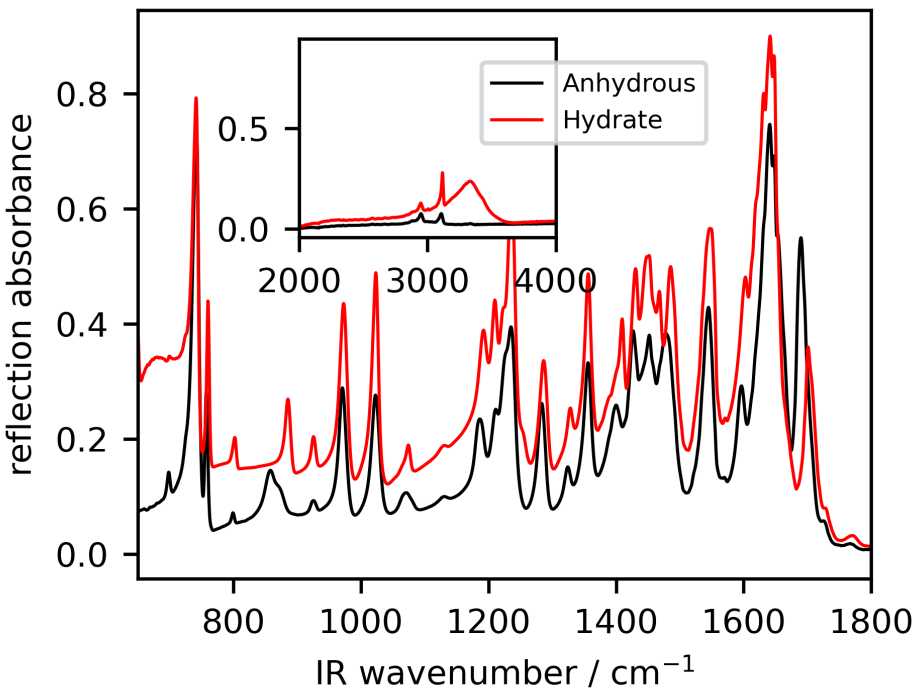

Figure 4.5: ATR–IR spectra, 650–1800 cm^{-1} of anhydrous and hydrated caffeine. The inset shows the 2000–4000 cm^{-1} spectral region.

include the shifting of the $C_{(8)}$–H out-of-plane deformation from a broad peak at 860 to a narrow peak at 888 cm^{-1} and the increased baseline below 750 cm^{-1} [66].

4.3 Analysis of Hydrated Illicit Opioids

Fig. 4.6 shows the IR spectra of five replicates of a 10% fentanyl binary standard that were prepared with the hydrated caffeine, the spectra of anhydrous and hydrated caffeine are also shown. It appears that the conversion to the hydrated form of caffeine was not complete, all five replicates show features of both forms of caffeine. Replicate #1 in Fig. 4.6 has the distinctive 888 and 3121 cm^{-1} of caffeine hydrate, as well this replicate shows the strongest absorbance in the O–H region and below 750 cm^{-1}. By contrast, replicate #5 in Fig. 4.6 looks like a mixture of anhydrous and hydrated caffeine, both the broad peak at 860 cm^{-1} and the narrow peak at 888 cm^{-1} are clearly visible. Even though only 30 mg of each standard was prepared there was noticeable variability in the degree of caffeine hydration among different aliquots of a single standard. Fig. 4.7 shows the accuracy line for the semi-hydrated binary standards using the robust PLSR model trained on the binary, heroin, mannitol and erythritol standards only. The fentanyl content was consistently over-predicted, the RMSEP was 5.8%, when the caffeine in illicit opioids was present as a mixture of anhydrous and hydrated caffeine. However, if both the anhydrous and semi-hydrated forms of caffeine are included in the training data the predicted fentanyl concentrations show improved accuracy, the RMSEP was 1.4%. Fig. 4.8 shows the accuracy line for the semi-hydrated binary standards using the robust PLSR model trained on the all five sets of standards: the anhydrous binary, semi-hydrated binary, heroin, mannitol and erythritol standards.

When LOF is repeated with the semi-hydrated standards in the training set the number of novelties in the service samples is reduced from 282 to 213. After excluding the anomalous samples identified by LOF and samples with negative predictions, 468 service samples from October 2018 to December 2020 remained. The mean fentanyl concentration

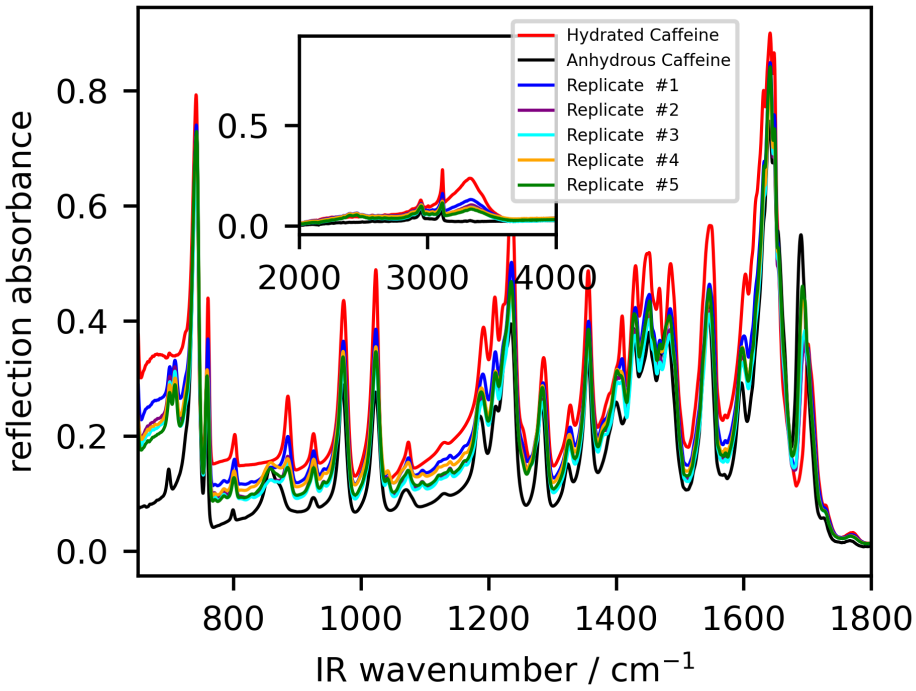

Figure 4.6: ATR–FTIR spectra, 650–1800 cm^{-1} of five replicates of a 10% fentanyl in semi-hydrated caffeine standard spectra, the spectra of anhydrous and hydrated caffeine are shown in black and red respectively. The inset shows the 2000–4000 cm^{-1} spectral region.

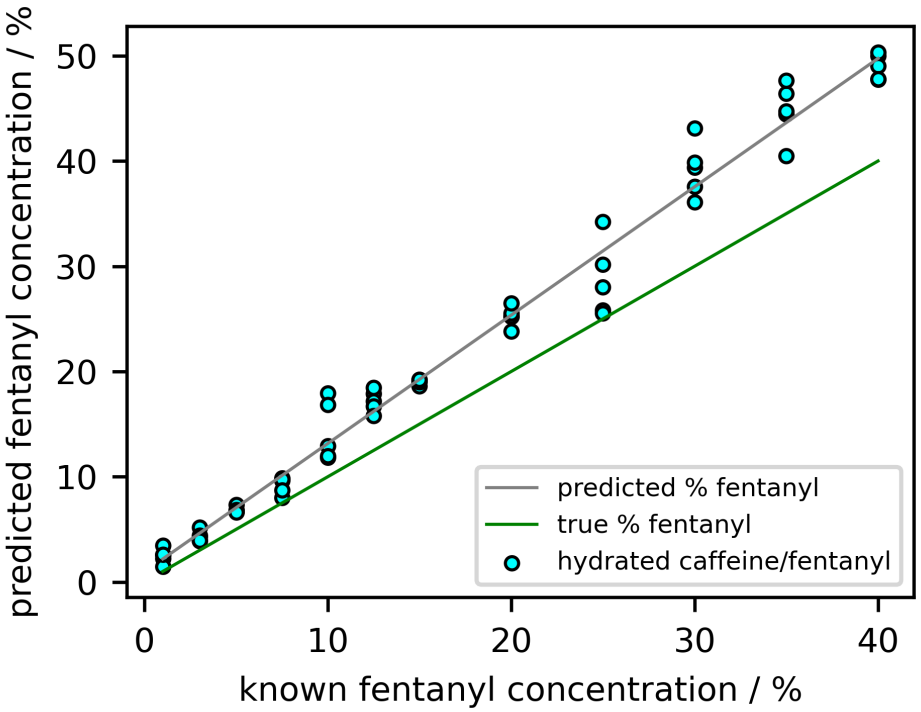

Figure 4.7: Accuracy line for the semi-hydrated binary standards for the robust PLSR model trained on the binary, heroin, mannitol and erythritol standards only. The spectral range of 650–3250 cm^{-1} was selected, 3 and 5 replicates were in the calibration and test sets respectively, and 10 fold cross validation was used.

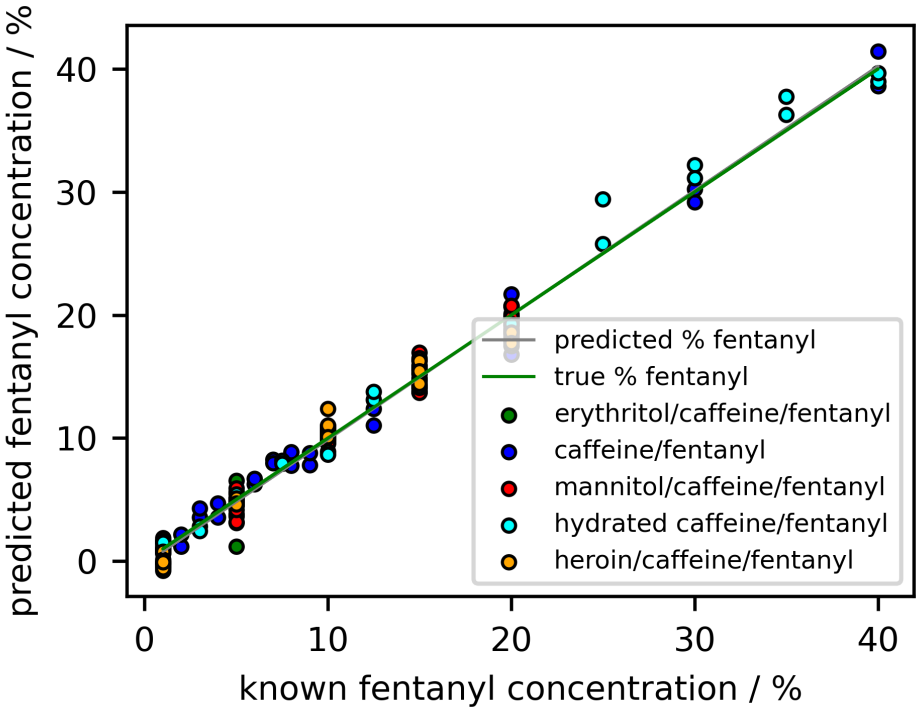

Figure 4.8: Accuracy line for the semi-hydrated binary standards for the robust PLSR model, trained on all five sets of standards: anhydrous binary, semi-hydrated binary, heroin, mannitol and erythritol standards. The spectral range of 650–3250 cm^{-1} was selected, 3 and 2 replicates were in the calibration and test sets respectively, and 10 fold cross validation was used.

was found to be 9% with a standard deviation of 7%. When the same analysis was performed without the semi-hydrated standards, Fig. 3.13, the mean fentanyl concentration was 10% with a standard deviation of 7%.

4.4 Conclusions

Illicit opioids which contained caffeine hydrate were discovered upon examination of the novelties identified by LOF. The IR spectrum of caffeine shows subtle changes upon its hydration, which are due to differences in the hydrogen bonding pattern of the two forms of caffeine. When semi-hydrated caffeine was combined into binary standards with fentanyl HCl these spectral changes interfered with the robust PLSR model's ability to accurately quantify fentanyl content. However, when the semi-hydrated standards are included in the PLSR training set then the model's accuracy was significantly improved.

Chapter 5

Conclusions

5.1 Summary of Work

Community drug checking data was collected by the Vancouver Island Drug Checking Project. Drug samples were analyzed using a variety of methods including fentanyl and benzodiazepine immunoassay test strips, ATR–FTIR spectroscopy, Raman spectroscopy, and gas chromatography coupled with mass spectrometry.

The analyzed illicit opioids were often mixtures of powdered fentanyl and cutting agents. Caffeine, mannitol, heroin, and erythritol were the most commonly identified components in fentanyl positive opioid samples. Based on these results representative binary and ternary opioid standards were prepared.

The IR spectra of the standards were used to build and test partial least squares regression models to quantify the fentanyl content. A grid search was used to comprehensively optimize the data preprocessing strategy and the number of latent variables used in the PLSR model. This optimization process was done for all the sets of standards (binary, mannitol, erythritol and heroin) individually and combined into one model, known as the robust model. A robust PLSR model is desirable from a service perspective since it is not always possible to reliably identify all components in an illicit opioid sample and the binary model was shown to give erroneous fentanyl predictions when an additional component is present in the sample. The extent of predictive error was dependant on both the identity of the additional component and the relative amount of this component. The optimized robust

PLSR model was able to accurately quantify fentanyl with an average RMSEP value of 1.10%.

Prior to a large scale analysis of the fentanyl content in illicit opioids, anomalous samples were identified by LOF and excluded. 425 service samples from October 2018 to December 2020 remained were quantified using the robust PLSR model. There was considerable variability in the fentanyl concentration in the samples, the mean was found to be 10% with a standard deviation of 7%.

Examination of the novelties identified by LOF analysis led to the discovery of illicit opioid samples in which the caffeine was present as caffeine hydrate instead of anhydrous caffeine. Caffeine is a solvate, and can reportedly undergo hydration by recrystallization or mechanochemistry in presence of water. The water of crystallization alters caffeine's hydrogen bonding pattern which causes subtle changes in the IR spectra of the two caffeine forms.

Attempts to hydrate an anhydrous caffeine standard showed a varying degree of success, the resultant caffeine ranged from semi-hydrated to fully hydrated depending on which aliquot of powder was analyzed by IR spectroscopy. When the robust PLSR model, trained on anhydrous caffeine standards only, was used to quantify the semi-hydrated binary standards the fentanyl content was overpredicted. However, if the semi-hydrated standards are also included in the training set for the PLSR model then the accuracy of the fentanyl quantification is improved.

5.2 Future Work

It is important to continue to expand the types of standards that are included in the robust model. A start would be to create new standards based on the anomalous service samples that were identified by LOF, including samples with high concentrations of fentanyl or heroin and mixtures of fentanyl and sugar alcohols. As well, the analysis from Chapter 4 should be repeated with completely hydrated caffeine to fully investigate the effect of

caffeine hydration on fentanyl quantification in illicit opioids.

It is also of great interest to ascertain if the PLSR models are capable of quantifying fentanyl analogues. As well, since some illicit opioids are known to contain more than one analogue of fentanyl assessing how the models are affected by the presence of multiple fentanyl species is recommended.

References

[1] "National Harm Reduction Coalition", https://harmreduction.org, Accessed: 2021-02-01.

[2] "Harm Reduction International", https://www.hri.global/what-is-harm-reduction, Accessed: 2021-02-01.

[3] Barratt, M. J.; Kowalski, M.; Maier, L. J.; Ritter, A. "Global Review of Drug Checking Services Operating in 2017", Technical Report, National Drug and Alcohol Research Centre, 2018.

[4] Brunt, T. "Drug Checking as a Harm Reduction Tool for Recreational Drug Users: Opportunities and Challenges", Technical Report, Drug Information and Monitoring System, 2017.

[5] Brunt, T. M.; Nagy, C.; Bucheli, A.; Martins, D.; Ugarte, M.; Beduwe, C.; Vilamala, M. V. *Drug Test. Anal.* **2017,** *9*, 188–198.

[6] Harper, L.; Powell, J.; Pijl, E. M. *Harm Reduct. J* **2017,** *14*, 52.

[7] Sorak, D.; Herberholz, L.; Iwascek, S.; Altinpinar, S.; Pfeifer, F.; Siesler, H. W. *Appl. Spectrosc. Rev.* **2012,** *47*, 83–115.

[8] Karila, L.; Billieux, J.; Benyamina, A.; Lancon, C.; Cottencin, O. *Brain Res. Bull.* **2016,** *126*, 61–67.

[9] Bardwell, G.; Kerr, T. *Subst. Abuse Treat. Prev. Policy* **2018,** *13*, 20.

[10] Laing, M. K.; Tupper, K. W.; Fairbairn, N. *Int. J. Drug Policy* **2018,** *62,* 59–66.

[11] Walczak, J. J.; Wang, L.; Bardy, S. L.; Feriancikova, L.; Li, J.; Xu, S. *Colloids Surf., B* **2012,** *90,* 129–136.

[12] Fairbairn, N.; Coffin, P. O.; Walley, A. Y. *Int. J. Drug Pol.* **2017,** *46,* 172–179.

[13] Kerr, T.; Mitra, S.; Kennedy, M. C.; McNeil, R. *Harm Reduct. J* **2017,** *14,* 28.

[14] "Government of Canada; Supervised Conumption Sites: Status of Application", `https://www.canada.ca/en/health-canada/services/substance-use/supervised-consumption-sites/status-application.html#wb-auto-4`, Accessed: 2021-02-01.

[15] Smolina, K.; Crabtree, A.; Chong, M.; Zhao, B.; Park, M.; Mill, C.; Schutz, C. G. *Drug Alcohol Depend.* **2019,** *194,* 151–158.

[16] Tupper, K. W.; McCrae, K.; Garber, I.; Lysyshyn, M.; Wood, E. *Drug Alcohol Depend.* **2018,** *190,* 242–245.

[17] Krieger, M. S.; Goedel, W. C.; Buxton, J. A.; Lysyshyn, M.; Bernstein, E.; Sherman, S. G.; Rich, J. D.; Hadland, S. E.; Green, T. C.; Marshall, B. D. L. *Int. J. Drug Policy* **2018,** *61,* 52–58.

[18] Oh, H.; Kim, K.; Miller, D.; Veloso, D.; Lin, J.; McFarland, W. *Int. J. Drug Policy* **2020,** *82,* 102787.

[19] Peiper, N. C.; Clarke, S. D.; Vincent, L. B.; Ciccarone, D.; Kral, A. H.; Zibbell, J. E. *Int. J. Drug Policy* **2019,** *63,* 122–128.

[20] Wallace, B.; van Roode, T.; Pagan, F.; Phillips, P.; Wagner, H.; Calder, S.; Aasen, J.; Pauly, B.; Hore, D. *Harm. Reduct. J* **2020,** *17,* 29.

[21] Weicker, N. P.; Owczarzak, J.; Urquhart, G.; Park, J. N.; Rouhani, S.; Ling, R.; Morris, M.; Sherman, S. G. *Int. J. Drug Policy* **2020,** *84,* 102900.

[22] Goldman, J. E.; Waye, K. M.; Periera, K. A.; Krieger, M. S.; Yedinak, J. L.; Marshall, B. D. L. *Harm Reduct. J.* **2019,** *16,* 3.

[23] BTNX, "Fentanyl Strips for Harm Reduction Use", Technical Report, Markham, Ontario, 2020.

[24] Karamouzian, M.; Dohoo, C.; Forsting, S.; McNeil, R.; Kerr, T. *Harm Reduct. J* **2018,** *15,* 46.

[25] Glick, J. L.; Christensen, T.; Park, J. N.; McKKenzie, M.; Green, T. C.; Sherman, S. G. *Drug Alcohol Depend.* **2019,** *194,* 527–532.

[26] Karamouzian, M.; Papamihali, K.; Graham, B.; Crabtree, A.; Mill, C.; Margot, K.; Sara, Y.; Buxton, J. A. *Int. J. Drug Policy* **2020,** *77,* 102665.

[27] Green, T. C.; Park, J. N.; Gilbert, M.; McKenzie, M.; Struth, E.; Lucas, R.; Clarke, W.; Sherman, S. G. *Int. J. Drug Policy* **2020,** *77,* 102661.

[28] Maghsoudi, N. *et al. Harm Reduct. J.* **2020,** *17,* 9.

[29] Centre on Drug Policy Evaluation, "Comparing Models of Drug Checking Services in Canada", Technical Report, Toronto, Ontario, 2018.

[30] Borden, S. A.; Saatchi, A.; Krogh, E. T.; Gill, C. G. *Anal. Sci. Adv.* **2020,** *7,* 97–108.

[31] McCrae, K.; Tobias, S.; Grant, C.; Lysyshyn, M.; Laing, R.; Wood, E.; Ti, L. *Drug Alcohol Rev.* **2020,** *39,* 98–102.

[32] Ti, L.; Tobias, S.; Lysyshyn, M.; Laing, R.; Nosova, E.; Choi, J.; Arredondo, J.; McCrae, K.; Tupper, K.; Wood, E. *Drug Alcohol Depend.* **2020,** *212,* 108006.

[33] Palamar, J. J.; Salomone, A.; Barratt, M. J. *Curr. Opin. Psychiatry* **2020,** *33,* 301–305.

[34] Milosevic, M. *Internal Reflection and ATR Spectroscopy;* John Wiley & Sons, Inc.: Hoboken, NJ, 2012.

[35] Mirabella, F. M. *Internal Reflection Spectroscopy; Theory and Applications;* Marcel Dekker, Inc.: New York, NY, 2013.

[36] Stuart, B. H. *Infrared Spectroscopy: Fundamentals and Applications;* John Wiley & Sons, Inc.: Hoboken, NJ, 2004.

[37] Pedregosa, F. *et al. J. Mach. Learn. Res.* **2011,** *12,* 2825–2830.

[38] Wold, S.; Sjostrom, M.; Eriksson, L. *Chemom. Intell. Lab. Syst.* **2001,** *58,* 109–130.

[39] Karunathilaka, S. R.; Mossoba, M. M.; Chung, J. K.; Haile, E. A.; Srigley, C. T. *J. Agric. Food Chem.* **2017,** *65,* 224–233.

[40] Hirri, A.; Bassbasi, M.; Souhassou, S.; Kzaiber, F.; Oussama, A. *Int. J. Food Prop.* **2016,** *19,* 1504–1512.

[41] Anjos, O.; Campos, M. G.; Ruiz, P. C.; Antunes, P. *Food Chem.* **2015,** *169,* 218–223.

[42] Koch, C.; Posch, A. E.; Goicoechea, H. C.; Herwig, C.; Lendl, B. *Anal. Chim. Acta* **2014,** *807,* 103–110.

[43] Algethami, F. K.; Eid, S. M.; Kelani, K. M.; Elghobashy, M. R.; Abd El-Rahman, M. K. *RSC Adv.* **2020,** *10,* 7146–7154.

[44] Groberio, T. S.; Zacca, J. J.; Botelho, E. D.; Talhavini, M.; Braga, J. W. B. *Forensic Sci. Int.* **2015,** *257,* 297–306.

[45] Lee, L. C.; Liong, C.-Y.; Jemain, A. A. *Chemom. Intell. Lab. Syst.* **2017,** *163,* 64–75.

[46] Mas, C.; Rubio, L.; Valverde-Som, L.; Sarabia, L. A.; Ortiz, M. C. *Chemom. Intell. Lab. Syst.* **2020,** *201*, 104006.

[47] Gerretzen, J.; Szymanska, E.; Jansen, J. J.; Bart, J.; van Manen, H.-J.; van den Heuvel, E. R.; Buydens, L. M. C. *Anal. Chem.* **2015,** *87,* 12096–12103.

[48] Engel, J.; Gerretzen, J.; Szymanska, E.; Jansen, J. J.; Downey, G.; Blanchet, L.; Buydens, L. M. C. *Trends Anal. Chem.* **2013,** *50,* 96–106.

[49] Rinnan, A.; van der Berg, F.; Engelson, S. B. *Trends Anal. Chem.* **2009,** *28,* 1201–1222.

[50] Esquerre, C.; Gowen, A. A.; Burger, J.; Downey, G.; O'Donnell, C. P. *Chemom. Intell. Lab. Syst.* **2012,** *117,* 129–137.

[51] De Luca, M.; Ioele, G.; Spatari, C.; Ragno, G. *J. Pharm. Biomed. Anal.* **2017,** *134,* 346–351.

[52] Long, V.; Tobias, S.; Lysyshyn, M.; Sage, C.; Bridgeman, J.; Gibson, E.; Laing, R.; Arredondo, J.; Patel, P.; Matthews, J.; Pearce, H.; Buxton, J.; Ti, L. "A Report on British Columbia's Unregulated Drug Supply: Results from British Columbia's Community Drug Checking Service, June 2018–December 2019", Technical Report, Vancouver, BC, 2020.

[53] Smith, B. C. *Spectroscopy* **2016,** *31,* 36–39.

[54] Asadi, Z.; Esrafili, M. D.; Vessally, E.; Asnaashariisfahani, M.; Yahyaei, S.; Khani, A. *J. Mol. Struct.* **2017,** *1128,* 552–562.

[55] Tamburini, E.; Vincenzi, F.; Costa, S.; Mantovi, P.; Pedrini, P.; Castaldelli, G. *Sensors* **2017,** *17,* 2366.

[56] Planinsek, O.; Planinsek, D.; Zega, A.; Breznik, M.; Srcic, S. *Int. J. Pharm.* **2006,** *319,* 13–19.

[57] Udvardi, B.; Kovacs, I. J.; Fancsik, T.; Konya, P.; Batori, M.; Stercel, F.; Falus, G.; Szalai, Z. *Appl. Spectrosc.* **2017,** *71*, 1157–1168.

[58] Tobias, S.; Wu, A. M. S. H.; Ti, L. *Can. J. Addiction* **2020,** *11*, 28–32.

[59] Health Canada, "Analyzed Drug Report: Canada 2020—Q1 (January to March)", Technical Report, Ottawa, Ontario, 2020.

[60] Health Canada, "Analyzed Drug Report: Canada 2020—Q2 (April to June)", Technical Report, Ottawa, Ontario, 2020.

[61] Health Canada, "Analyzed Drug Report: Canada 2020—Q3 (July to September)", Technical Report, Ottawa, Ontario, 2020.

[62] BC Centre for Disease Control, "Etizolam in British Columbia's Illicit Drug Market", Technical Report, Vancouver, BC, 2021.

[63] BC Coroners Service, "Illicit Drug Toxicity Deaths in BC", Technical Report, Ministry of Public Safety & Soliciter General, Victoria, BC, 2020.

[64] Laing, R. "Fentanyl in Street Samples and Drug Checking Trends", Technical Report, Ottawa, Ontario, 2020.

[65] Gonzalez-Gonzalez, J. S.; Zuniga-Lemus, O.; del Carmen Hernandez-Galindo, M. *IOSR J. Pharm.* **2017,** *7*, 28–30.

[66] Nolasco, M. M.; Amado, A. M.; Ribeiro-Claro, P. J. A. *ChemPhysChem* **2006,** *7*, 2150–2161.